HEPATOLOGY
Official Journal of the American Association for the Study of Liver Diseases

# Reversal of Hepatocyte Senescence After Continuous *In Vivo* Cell Proliferation

Min-Jun Wang,[1,2]* Fei Chen,[1,2]* Jian-Xiu Li,[1,2] Chang-Cheng Liu,[1,2] Hai-Bin Zhang,[3] Yong Xia,[3] Bing Yu,[1,2] Pu You,[1,2] Dao Xiang,[1,2] Lian Lu,[1,2] Hao Yao,[1,2] Uyunbilig Borjigin,[4] Guang-Shun Yang,[3] Kirk J. Wangensteen,[5] Zhi-Ying He,[1,2] Xin Wang,[4,6,7] and Yi-Ping Hu[1,2]

**A better understanding of hepatocyte senescence could be used to treat age-dependent disease processes of the liver. Whether continuously proliferating hepatocytes could avoid or reverse senescence has not yet been fully elucidated. We confirmed that the livers of aged mice accumulated senescent and polyploid hepatocytes, which is associated with accumulation of DNA damage and activation of p53-p21 and $p16^{ink4a}$-pRB pathways. Induction of multiple rounds continuous cell division is hard to apply in any animal model. Taking advantage of serial hepatocyte transplantation assays in the fumarylacetoacetate hydrolase-deficient ($Fah^{-/-}$) mouse, we studied the senescence of hepatocytes that had undergone continuous cell proliferation over a long time period, up to 12 rounds of serial transplantations. We demonstrated that the continuously proliferating hepatocytes avoided senescence and always maintained a youthful state. The reactivation of telomerase in hepatocytes after serial transplantation correlated with reversal of senescence. Moreover, senescent hepatocytes harvested from aged mice became rejuvenated upon serial transplantation, with full restoration of proliferative capacity. The same findings were also true for human hepatocytes. After serial transplantation, the high initial proportion of octoploid hepatocytes decreased to match the low level of youthful liver. *Conclusion:* These findings suggest that the hepatocyte "ploidy conveyer" is regulated differently during aging and regeneration. The findings of reversal of hepatocyte senescence could enable future studies on liver aging and cell therapy. (HEPATOLOGY 2014;00:000-000)**

As with other body organs, the liver undergoes a process of aging. The aging liver has been reported to gradually decrease in size and in total numbers of hepatocytes, decrease in regenerative and metabolic capacity, and increase in proportion of polyploid hepatocytes.[1-3] Generally, all organs accumulate senescent cells with aging.[4,5] Cellular senescence typically is characterized by telomere shortening or telomere dysfunction,[6,7] activation of genes at the INK4a/ARF locus,[8,9] and accumulation of DNA damage.[4,10,11] Two main tumor suppressor pathways, p53-p21 and $p16^{ink4a}$-pRB, become activated when cells enter into senescence.[4,5,12] Some of the parameters commonly used to identify senescent cells *in vitro* and *in vivo* include SA-$\beta$-GAL activity, blockage of cell proliferation, cell enlargement, accumulation of DNA damage with accumulation of histone $\gamma$-H2A.X foci, and increased levels of cell cycle inhibitors $p16^{INK4A}$, p21, and p53.[8,13] At present, no marker or hallmark of senescence has been found to be entirely specific to

*Abbreviations: Alb, albumin; FAH, fumarylacetoacetate hydrolase; FACS, fluorescent activated cell sorting; NTBC, 2-(2-nitro-4-trifluoromethylbenzoyl)-1,3-cyclohexanedione.*

*From the [1]Department of Cell Biology, Second Military Medical University, Shanghai, P.R. China; [2]Center for Stem Cell and Medicine, Graduate School, Second Military Medical University, Shanghai, P.R. China; [3]Eastern Hepatobiliary Surgery Hospital, Second Military Medical University, Shanghai, P.R. China; [4]Key Laboratory of National Education Ministry for Mammalian Reproductive Biology and Biotechnology, Inner Mongolia University, Huhhot, P.R. China; [5]Department of Medicine, Division of Gastroenterology, University of Pennsylvania, Philadelphia, PA, USA; [6]Department of Laboratory Medicine and Pathology, University of Minnesota, Minneapolis, MN, USA; [7]Hepatoscience Inc, Palo Alto, CA, USA.*

*Received September 9, 2013; accepted February 20, 2014.*

*Funded by National Key Basic Research and Development Program of China (2011CB966200, 2010CB945600), National Natural Science Foundation of China (31271474, 31171309, 30971462, 31271469, 31271042, and 31100996).*

**These authors contributed equally to this work.*

*Present address for Pu You, Dao Xiang: Naval Medical Research Institute, Shanghai 200433, P.R. China.*

the senescence state, and not all senescent cells express all of these senescent markers. Cellular senescence was once regarded as an irreversible process, permanently blocking an aging cell from entering the cell cycle.[4] However, many recent findings describe instances where senescence can be reversed.[12,14-17]

The liver is different from many other organs for its specific capacity to regenerate. Previous findings revealed that mouse hepatocytes could undertake at least 86 cell doublings after seven rounds of transplantation.[18] The repopulating hepatocytes after the seventh round of serial transplantation still carried a normal capacity of liver repopulation without reaching an upper limit of cell divisions.[18] Human hepatocytes and cholangiocytes in normal liver maintain a constant telomere length with increasing age,[19] suggesting that human liver cells may be similar to mouse liver cells in maintaining the potential to proliferate and avoid senescence. Interestingly, senescent hepatocytes from severely cirrhotic mouse livers could recover both proliferative capacity and physiological functions when transplanted into livers of normal young recipients, which strongly suggests that hepatocyte senescence might be reversed by uncharacterized factors in the microenvironment of normal liver.[20] However, hepatocyte senescence itself has not been completely characterized in previous studies.

Neither has the relationship between hepatic senescence and hepatic polyploidy been fully explored. The accumulation of polyploid hepatocytes with age was previously regarded as the accumulation of hepatocytes that fail to undergo cytokinesis of cell division.[21-23] Hepatocyte polyploidy has also been regarded as cellular senescence.[21] However, a recent finding reported the existence of a hepatocyte "ploidy conveyor," which may be actively preserved throughout hepatocyte development and maturation.[24] Polyploidization together with aneuploidy is thought to be a conserved source of genetic variation with hepatocytes, which allows animals to survive injuries to the liver such as from environmental toxins.[24,25] Whether the activity of the ploidy conveyor is maintained during hepatocyte proliferation has not yet been studied.

In this study we first defined the properties of cellular senescence and the ploidy of hepatocytes in normal mouse liver over 18 months of age. We isolated hepatocytes from either 2-month-old or 18-month-old mouse livers and performed serial transplantation. We found that both young and aged hepatocytes inhibit senescence programs upon regeneration. After serial transplantation and serial liver repopulation the proportion of hepatocytes at each level of ploidy (diploid, tetraploid, or octoploid) returned to the levels of the youthful state, suggesting that the "ploidy conveyer" may be activated differently with age and regeneration. Finally, human hepatocytes, similar to mouse counterparts, also rejuvenated by reversing senescence to recover proliferation capacity upon stimulation of liver repopulation.

## Materials and Methods

***Hepatocyte Isolation, Cell Transplantation, Serial Transplantation, and Repopulation Assay.*** Hepatocytes were isolated from livers of male 129S4 wild-type mice and Rosa26R-LacZ transgenic mice. Isolated hepatocytes were injected intrasplenically into $Fah^{-/-}$ mice as described previously.[26,27] Serial transplantations were performed as described previously.[18] Liver repopulated hepatocytes with $\beta$-gal expression were detected and sorted using the FluoReporter lacZ Flow Cytometry Kit (Invitrogen, Carlsbad, CA). Hepatocytes were retransplanted into fresh $Fah^{-/-}$ recipients. After 8 weeks of repopulation, the next round of transplantation was performed, and so on, up to 12 times. Livers were harvested and immunohistochemistry assay with fumarylacetoacetate hydrolase (FAH) antibody was used to examine the percentage of liver repopulation as described previously.[28-30] Human liver tissue was obtained from surgical resection specimens of patients with hepatic hemangioma (see Supporting Table S1 for patient characteristics). Isolation and transplantation of human hepatocytes was performed as described previously.[27] Experiments were approved by the Ethical Committee on Ethics of Biomedicine Research, Second Military Medical University, P.R. China.

*Address reprint requests to: Yiping Hu, Ph.D., Zhiying He, Ph.D., Department of Cell Biology, Second Military Medical University, 800 Xiangyin Road, Shanghai 200433, P.R. China. E-mail: yphu@smmu.edu.cn, zyhe@smmu.edu.cn; fax: +86-21-8187-0948; or Xin Wang, Ph.D., Key Laboratory of National Education Ministry for Mammalian Reproductive Biology and Biotechnology, Inner Mongolia University, Huhhot010021, P.R. China. E-mail: wangxin_cn@imu.edu.cn; fax: +86-0471-4994-329.*



*View this article online at wileyonlinelibrary.com.*

*DOI 10.1002/hep.27094*

*Potential conflict of interest: Nothing to report.*

***Flow Cytometry and Fluorescent Activated Cell Sorting (FACS).*** To quantify ploidy profiling, fixed hepatocytes were stained with propidium iodide (Sigma-Aldrich, St. Louis, MO) supplemented with RNAse A (Sigma-Aldrich), then performed by a FACS-Calibur flow cytometer (BD Biosciences, San Jose, CA). For isolation of hepatocyte with different ploidy, hepatocytes were incubated with Hoechst 33342 (Sigma-Aldrich) and sorted with an InFlux flow cytometer (Becton Dickinson, Franklin Lakes, NJ) using a 150-$\mu$m nozzle as described.[24]

Additional Materials and Methods can be found in the Supporting Material online.

## Results

***Hepatocyte Polyploidy Increases With Liver Age but Does Not Equate With Hepatocyte Senescence.*** Hepatocytes in the adult liver normally turn over rarely (1-2 times/year), and therefore are generally quiescent.[31] We examined the dynamic process of hepatocyte senescence in normal mouse liver over the course of 18 months of life. Enlarged hepatocytes were evident in 18-month-old mice compared to 2-month-old mice (Supporting Fig. S1A). The results revealed that the percentages of SA-$\beta$-gal-positive and $\gamma$-H2A.X-positive hepatocytes increased with age from $1.37 \pm 0.64\%$ and $1.73 \pm 0.23\%$, respectively, at 2 months of age, to $10.55 \pm 0.78\%$ and $8.33 \pm 1.36\%$ at 12 months and to $40 \pm 4.6\%$ and $42.67 \pm 3.51\%$ at 18 months (Fig. 1A; Fig. S1B,C). The expression levels of $p16^{ink4a}$ and p21 increased significantly from 2 to 18 months (Fig. S1D). Similar to *in vivo* hepatocytes, cultured primary hepatocytes from 18-month-old mice had more SA-$\beta$-gal-positive cells and fewer of bromodeoxyuridine (BrdU)-positive cells than from 2-month-old mice, indicting that hepatocytes from older mice are more likely to be senescent and are less capable of proliferation (Fig. S1E,F).

Although it has been reported previously that the proportion of polyploidy hepatocytes increases continuously with age,[21] the relationship between polyploidy and senescence in hepatocytes had not been fully elucidated. We first examined the ploidy of hepatocytes, and found that the percentage of diploid cells gradually decreased from $23.40 \pm 3.05\%$ at 2 months of age to $15.47 \pm 1.33\%$ at 12 months, and $13.16 \pm 0.66\%$ at 18 months (Fig. S2A). In contrast, the proportion of octoploid hepatocytes doubled from 2 months to 18 months from $16.80 \pm 5.1\%$ to $34.06 \pm 1.80\%$ (Fig. S2A).

We next purified diploid, tetraploid, and octoploid hepatocytes from 2- and 18-month-old mice by FACS based on DNA content (Fig. 1B).[24] We found that expression levels of $p16^{ink4a}$, p21, and p53 in diploid, tetraploid, and octoploid hepatocytes from 18-month-old mice were all higher than those from 2-month-old mice (Fig. 1C; S2B). Moreover, expression levels of $p16^{ink4a}$, p21, and p53 in octoploid hepatocytes from 18-month-old mice were also much higher than those of diploid and tetraploid hepatocytes from the same mice (Fig. 1C; S2B). In addition, the proportion of $\gamma$-H2A.X-positive cells was as low as about 2.5% of all hepatocytes at all three levels of ploidy in 2-month-old mice. It became $9.3 \pm 1.11\%$ of diploid hepatocytes, $24.23 \pm 3.36\%$ of tetraploid hepatocytes, and $78.23 \pm 4.14\%$ of octaploid hepatocytes in 18-month-old mice (Fig. S2C). These results indicted that the increasing proportion of octoploid cells in 18-month-old mice correlated with the increasing hepatocyte senescence.

Hepatocytes are generally mononucleated or multinucleated. It was still unclear whether or not the number of nuclei correlates with senescence. Microscopic analysis after F-actin and Hoechst 33342 stainings was used to measure the DNA content and to directly assess the ploidy of hepatocytes,[21,32] because FACS cannot separate cells based on the number of nuclei. Using fluorescence imaging technology, we found that the percentage of mononucleated polyploid ($\geq$4n) hepatocytes gradually increased from $29.13 \pm 1.24\%$ at 2 months of age to $34.09 \pm 0.89\%$ in livers at 12 months, and $35.83 \pm 0.78\%$ at 18 months (Fig. 1D). Similarly, the percentage of binucleated polyploid ($\geq 2 + 2n$) hepatocytes increased from $41.87 \pm 1.19\%$ in livers at 2 months, to $45.17 \pm 0.83\%$ at 12 months, and to $49.63 \pm 1.79\%$ at 18 months (Fig. 1D). These results indicated that the proportions of both binucleated and mononucleated polyploid hepatocytes increased with age. The relationships between senescence, ploidy, and number of nuclei per cell were further determined by SA-$\beta$-gal and $\gamma$-H2A.X staining. The results showed that the majority of $\gamma$-H2A.X-positive hepatocytes were either mononucleated polyploid ($38.27 \pm 1.8\%$), or binucleated polyploid ($42.6 \pm 1.93\%$) (Fig. 1F). The remainder of $\gamma$-H2A.X-positive hepatocytes were the minority populations of either mononucleated diploid hepatocytes or trinucleated polyploid hepatocytes. Furthermore, we found that 70% of $\gamma$-H2A.X-positive hepatocytes were also positive for SA-$\beta$-gal (Fig. 1E,F), suggesting that the increase of polyploid hepatocytes in older mice correlated with senescence regardless of whether the polyploid hepatocytes had one or two nuclei.

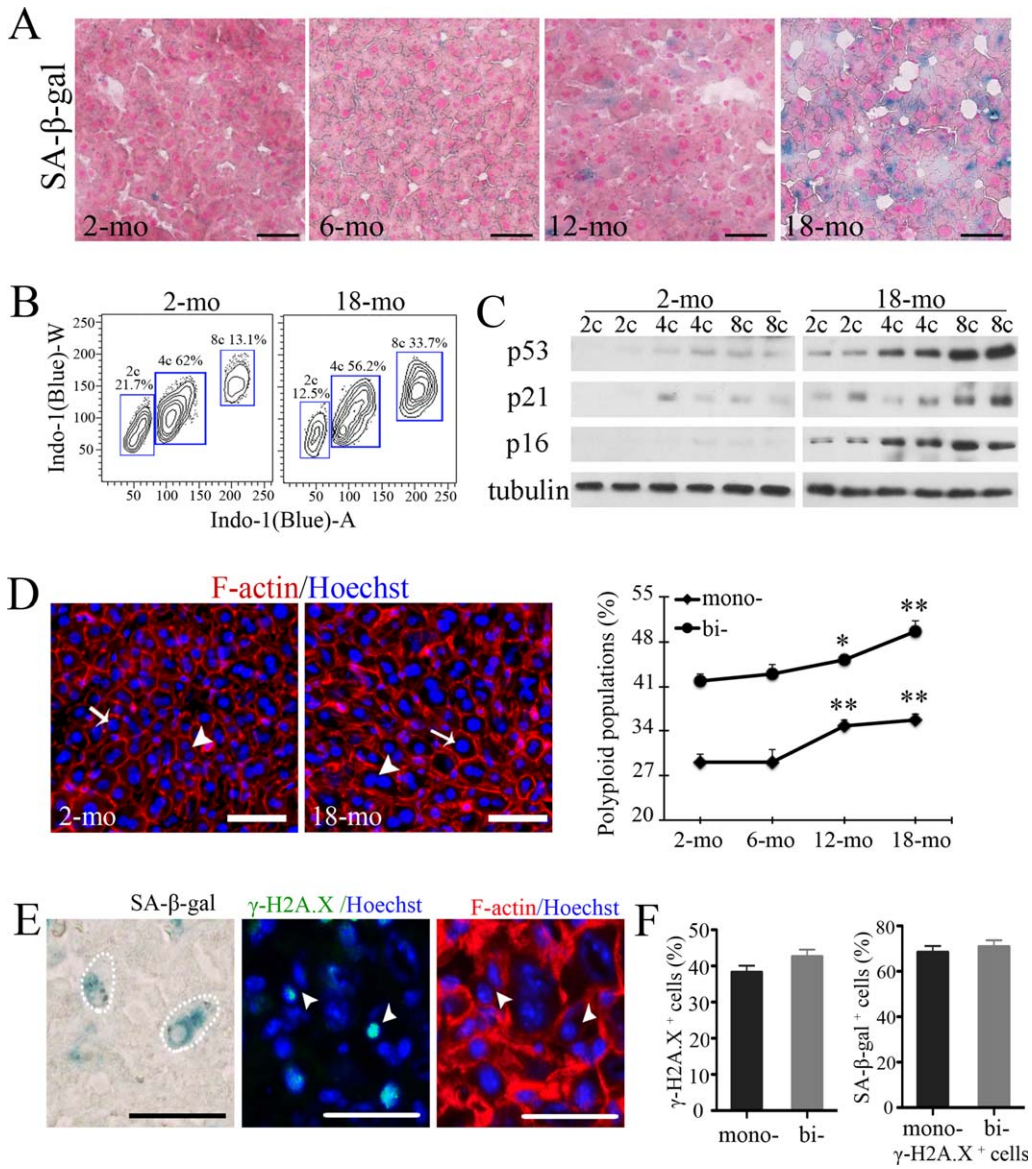


Fig. 1. Hepatocyte senescence and polyploidy. (A) Histochemistry assay for SA-$\beta$-gal activity in the liver of 2-, 6-, 12-, and 18-month-old mice (denoted 2-mo, 6-mo, 12-mo, and 18-mo, respectively). (B) Flow cytometry was used to analyze and sort highly pure 2c, 4c, and 8c hepatocytes from 2- and 18-month-old mice. (C) Western blot showing the protein levels of p16, p21, and p53 among three hepatocyte ploidy levels isolated from 2- and 18-month-old mice. (D) Representative liver sections stained by Hoechst (nuclear labeling) and Phalloidin (outline of a cell labeling, binding F-actin) at 2 and 18 months of age. The arrow marks representative mononucleated polyploid cells, while the arrowhead marks binucleated cells. The graph on the right shows the average percentage of mononucleated and binucleated polyploid populations. $^{*}P < 0.05$, $^{**}P < 0.01$ versus 2-month-old hepatocytes. (E) *In situ* analysis of 18-month-old liver sections showing DNA content and hepatocyte senescence based on expression of SA-$\beta$-gal and $\gamma$-H2A.X in the same sections. The left panel shows expression of SA-$\beta$-gal. The middle shows staining by $\gamma$-H2A.X and Hoechst. The right is double staining with Hoechst and F-actin. The white dashed lines and the arrowheads mark senescent cells. (F) Quantification of the percentage of mononuclear polyploid and multinuclear cells with expression of the senescence marker $\gamma$-H2A.X in 18-month-old hepatocytes (left). Quantification of the percentage of $\gamma$-H2A.X-positive polyploid cells that also express of SA-$\beta$-gal in 18-month-old liver (right). Shown are means $\pm$ SD. Scale bars = 40 $\mu$m.

In summary, we found that the proportion of both senescent and polyploid hepatocytes increases with age. Senescence did not necessarily equate with polyploidy; however, there was a fraction of diploid hepatocytes that were senescent, and vice versa, and a fraction of polyploid hepatocytes that were not senescent.

***Senescence Was Absent in the Hepatocytes Undergoing Continuous Cell Proliferation.*** We analyzed senescence in hepatocytes undergoing continuous proliferation during serial transplantations in $Fah^{-/-}$ mice, a mouse model of liver injury and repopulation. After the first liver repopulation, donor hepatocytes were reisolated and retransplanted into new recipients

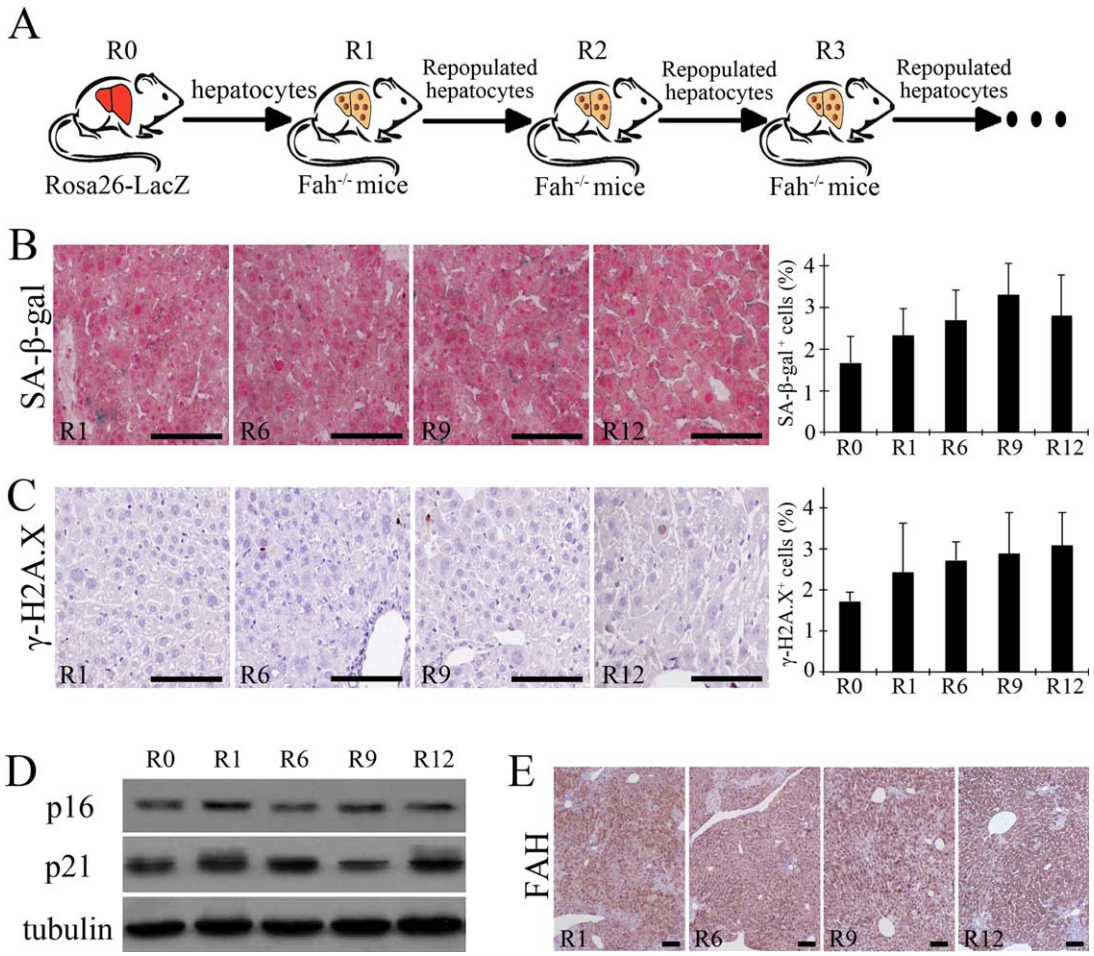


Fig. 2. Repopulated hepatocytes undergoing continuous cell proliferation maintain a youthful state. (A) Schema of serial transplantations for induction of continuous proliferation of hepatocytes *in vivo*. (B,C) Histochemistry assay showing activity of SA-$\beta$-gal (B) and immunohistochemistry staining for $\gamma$-H2A.X (C) in liver sections of primary and serially repopulated recipients 2 months after transplantation. Round 0, 1, 6, 9, 12 represents the number of rounds of serial transplantations. The panels on the right show quantification of number of cells with positive staining. (D) Western blot showing expression of p16and p21 in the livers of primary and serially repopulated recipients after transplantation. (E) Immunohistochemistry staining using FAH antibody of liver sections of recipients after serial transplantation showed equivalent proportion of the liver that was repopulated in recipients at 1, 6, 9, and 12 rounds of liver repopulation. Scale bars = 100 $\mu$m.

at each 8-week interval up to 12 times (Fig. 2A). The total time elapsed from birth of the original donor mouse was 26 months after 12 rounds of transplantation. As shown in Figs. 1 and S1, a significant amount of senescent hepatocytes, represented by either SA-$\beta$-gal or $\gamma$-H2A.X-positive, existed in the unmanipulated normal liver of 18-month-old mice. However, the percentages of either SA-$\beta$-gal or $\gamma$-H2A.X-positive hepatocytes remained very low at 1, 6, 9, and 12 rounds of transplantation (Fig. 2B,C), which were levels similar to 8-week-old, unmanipulated hepatocytes. Similarly, the expression levels of both $p16^{ink4a}$ and p21 in the repopulating hepatocytes after 12 rounds of transplantation were similar to those of 8-week-old hepatocytes (Fig. 2D). Remarkably, the repopulation capacity of hepatocytes did not diminish even after 12 rounds of transplantation, always keeping a consistent rate of more than 85% liver repopulation (Fig. 2E).

***Senescent Hepatocytes Become Rejuvenated After Continuous Cell Proliferation.*** To determinate whether senescent hepatocytes could rejuvenate after they reenter cell cycles, we transplanted three kinds of donor hepatocytes into $Fah^{-/-}$ recipients at 8-week-old: 1) hepatocytes from 2-month-old mice; 2) repopulated hepatocytes after 12 rounds of serial transplantation; 3) hepatocytes from 18-month-old mice. At 3 weeks post-transplantation, Fah staining revealed that all kinds of donor hepatocytes could engraft into liver parenchyma, and the number of repopulating colonies was not significantly different among the three groups (Fig. 3A,B). However, colonies from donor hepatocytes of 2-month-old mice and those repopulated hepatocytes after 12 rounds of serial transplantation typically consisted of

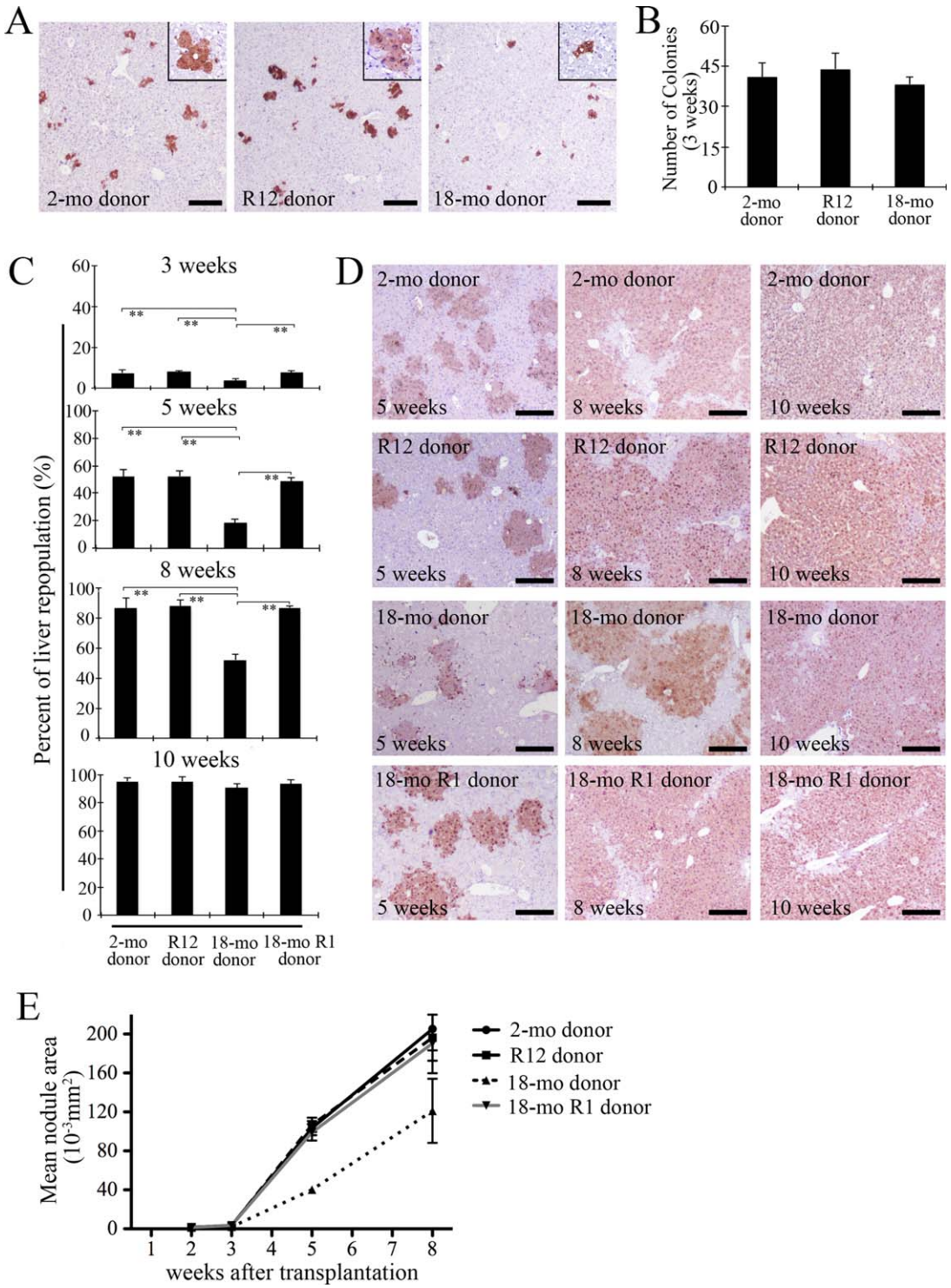


Fig. 3. Senescent hepatocytes rejuvenate to restore normal proliferative capacity. (A) Immunohistochemistry staining with FAH antibody to compare the capacities for engraftment and proliferation 3 weeks after transplantation of hepatocytes from 2-month-old mice, 12 rounds serially transplanted mice, and 18-month-old mice. Box: a magnified view. (B) Quantification of the numbers of Fah-positive nodules per visual field at 40-fold magnification in the three recipient groups. (C) Proportion of the liver that was repopulated in the four recipients groups after 3, 5, 8, 10 weeks. 2-mo, R12, 18-mo, and 18-mo R1 donors represent donor hepatocytes from: 2-month-old mice; 12 rounds of serially transplanted mice; 18-month-old mice; and one round serially transplanted mice with 18-month-old hepatocytes, respectively. (D) Representative sections showing FAH-positive staining of repopulating hepatocytes in the livers of the four recipient groups after 5, 8, 10 weeks. (E) A graph of the mean values of repopulation nodule area in liver sections after transplantation of hepatocytes isolated from 2-mo, R12, 18-mo and 18-mo R1 donors (mean ± SD). $*P < 0.05$; $**P < 0.01$. Scale bars = 200 $\mu$m.

4-5 hepatocytes, while the majority of colonies from donor hepatocytes of 18-month-old mice only consisted of 1-2 hepatocytes (Fig. 3A). The results indicated that donor hepatocytes from aged mice had a reduced proliferation capacity, although they could initially engraft into the liver parenchyma with efficiency equal to hepatocytes from younger or serially repopulated mice.

The efficiency of liver repopulation from the three kinds of donor hepatocytes was further examined at four timepoints in the following process. There was no significant difference between the percentages of liver repopulation by donor hepatocytes from either 2-month-old mice or repopulated hepatocytes after 12 rounds of serial transplantation at 3, 5, and 8 weeks of posttransplantation (Fig. 3C,D). In contrast, the percentage of liver repopulation and the nodule size from donor hepatocytes of 18-month-old mice at 3, 5, and 8 weeks posttransplantation were significantly lower or smaller than those finding results from experiments with the other two groups of hepatocytes (Fig. 3C-E). However, an equivalent rate of ~90% repopulation of the liver was achieved with all three groups of donor hepatocytes at 10 weeks posttransplantation (Fig. 3C,D), indicating that senescent hepatocytes from 18-month-old mice regained the potential to fully repopulate recipients after reentry into cell cycles.

Furthermore, hepatocytes were isolated from the recipients of 18-month-old hepatocytes at 10 weeks posttransplantation, and then serially retransplanted into the new $Fah^{-/-}$ recipients for 2 rounds. At 3, 5, and 8 weeks of the second round of serial transplantation, the percentage of liver repopulation from these hepatocyte donors was similar to the repopulation levels in recipients transplanted with donor hepatocytes from 2-month-old mice or the repopulated hepatocytes after 12 rounds of serial transplantation (Fig. 3C-E), indicating that the proliferation capacity of 18-month-old hepatocytes recovered to the full capacity of young hepatocytes after one round of transplantation and liver repopulation.

To further confirm that senescent hepatocytes could become rejuvenated after transplantation, three ploidy levels of hepatocytes were isolated from 2- or 18-month-old mice, and were transplanted into $Fah^{-/-}$ recipients of 8-week-old mice. The amount of repopulation nodules from the donor hepatocytes of 18 month-old mice, with various ploidies, was similar to those from the donor hepatocytes of 2 month-old mice, suggesting that they maintained an equivalent ability to engraft into liver parenchyma after transplantation (Fig. S3A; Fig. 4A,B). However, on examining the size of repopulation nodules, there was a significant reduction in size of nodules in recipients of polyploid hepatocytes from 18 month-old mice at 5 or 8 weeks posttransplantation, suggesting a low efficiency in repopulation up to these timepoints (Fig. 4C,D). There was no significant difference in the nodule size for any of the groups at 10 weeks posttransplantation, indicating that the older, polypoid hepatocyte donors eventually caught up with two other cell groups for capacity of liver repopulation (Fig. 4A,C). Remarkably, there was no significant difference among three kinds of donor hepatocytes from 2-month-old mice for the efficiency of liver repopulation, reflected from the percentage of liver repopulation and the mean nodule size at any checked timepoint (Fig. 4E; S3B-E).

More important, we found there was no significantly increased cell senescence in liver samples after one or two rounds of serial transplantation from the 18-month-old hepatocytes or the 18-month-old octoploid hepatocytes, shown in the SA-$\beta$-gal activity assay (Fig. 5A), $\gamma$-H2A.X staining (Fig. 5B), and in expression levels of $p16^{ink4a}$, p21, and p53 (Fig. 5C). In fact, levels of $p16^{ink4a}$, p21, and p53 gradually reduced during repopulation, while promoters of cell proliferation CDK2, CDK4, and pRB gradually increased (Fig. 5D). Telomere length was used as another critical marker of senescent cells to validate these findings.[7] We found that telomere shortening did not occur in hepatocytes up to 18 months and in donor hepatocytes undergoing serial transplantation and repopulation (Fig. 5E), which agreed with a previous report in human cells.[19] Interestingly, telomerase activity was reactivated in the repopulated hepatocytes (Fig. 5F) even though telomerase activity only existed in normal hepatocytes from 2-month-old mice. These results implied that restoration of telomerase activity during continuous hepatocyte proliferation was important for maintenance of the regenerative capacity of hepatocytes, and perhaps for avoidance of senescence.

A summary of the above data indicate that aged hepatocytes that originally expressed markers of senescence can become rejuvenated and reenter the cell cycle to repopulate the liver to the same degree as hepatocytes from youthful mice.

***Octoploid Hepatocytes Undergo Ploidy Reversal During Liver Repopulation.*** As mentioned above, the percentage of polyploid hepatocytes, especially octoploid ones, increased with age. However, after transplantation of hepatocytes from 18-month-old mice, repopulating hepatocytes harvested at 10 weeks posttransplantation were analyzed by flow cytometry. The results indicated that the ratio of diploid,

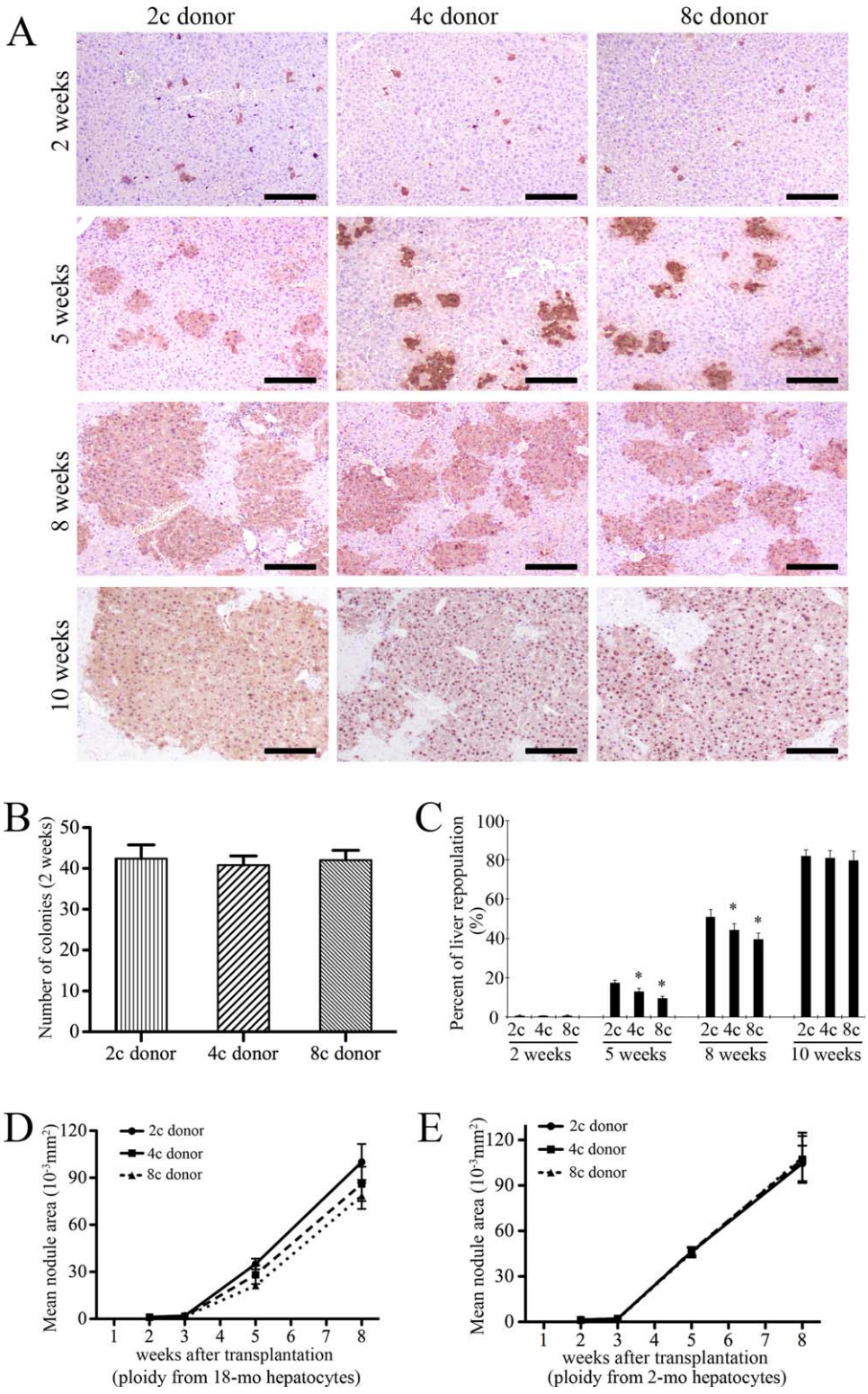


Fig. 4. Senescent polyploid hepatocytes can rejuvenate and repopulate the liver. (A) FAH immunohistochemistry staining was done to compare the capacity for engraftment and liver repopulation for hepatocytes from 18-month-old mice of 2c, 4c, and 8c DNA content at 2-, 5-, 8-, 10-weeks post-transplantation. 2c, 4c, and 8c represent diploid, tetraploid, and octoploid donor hepatocytes. (B) The number of Fah-positive clones was counted per visual field at 40-fold magnification in three recipient groups. (C) Proportion of the liver that was repopulated after transplantation of 2c, 4c, and 8c hepatocyte donors 2, 5, 8, and 10 weeks later. $*P < 0.05$ versus 2c hepatocytes. (D,E) Mean area of donor-derived nodules after transplantation of 2c, 4c, and 8c hepatocytes isolated from 18-month-old mice (D) and 2-month-old mice (E). The data are means ± SD. Scale bars = 200 $\mu$m.

tetraploid, and octoploid cells all became similar to that ratio seen in liver of 2-month-old mice (Fig. 6A). The percentage of octoploid hepatocytes decreased from 34.06 ± 1.80% before transplantation to 17.40 ± 0.96%, while the percentage of diploid hepatocytes increased from 13.16 ± 0.66% to 21.96 ± 1.78%. This distribution remained stable after a second round of serial transplantation (Fig. 6A).

In order to clarify whether ploidy reversal participated in the reduction of octoploid hepatocytes, separately isolated diploid, tetraploid, and octoploid hepatocytes from the recipient mice with a 12th round

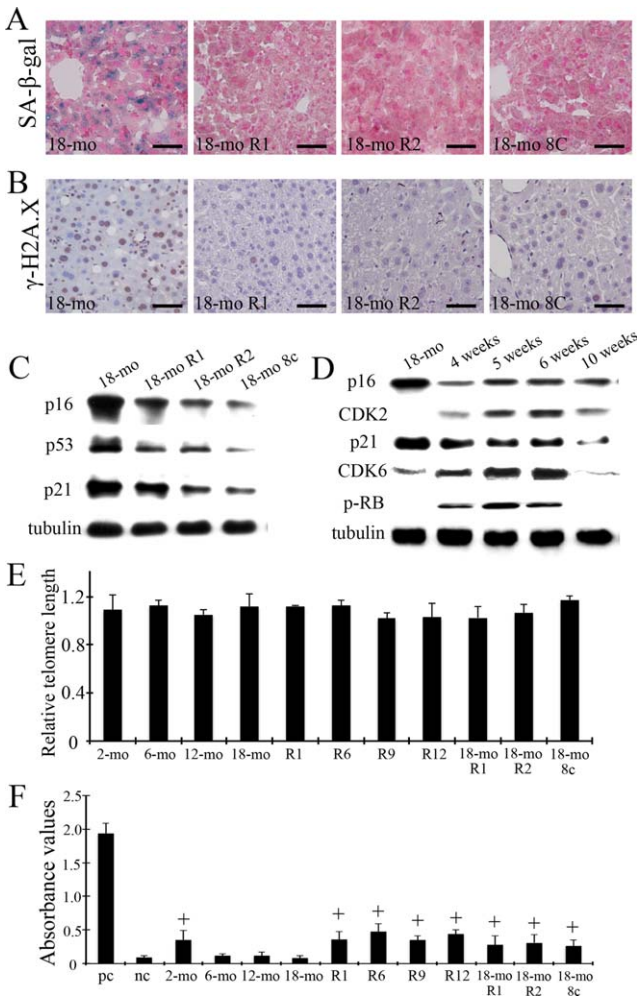


Fig. 5. Evaluation of cellular senescence after transplantation of aged hepatocytes. (A,B) Expression of SA-$\beta$-gal (A) and $\gamma$-H2A.X (B) was detected in 18-month-old liver sections (18-mo), recipients of 18-month-old hepatocytes after one round of liver repopulation (18-mo R1), recipients after two rounds of liver repopulation (18-mo R2) and recipients of sorted octoploid hepatocytes from 18-month-old mice after one round of liver repopulation (18-mo 8c). Scale bars = 50 $\mu$m. (C) Western blot showing the expression of p16, p21, and p53 in the livers of the four groups. (D) Western blot demonstrating the dynamic expression of p53-p21 and p16-RB pathway proteins in repopulated livers in the same four groups. (E) Results of a quantitative polymerase chain reaction (PCR) assay to measure telomere length of hepatocytes at the indicated ages and stages of serial repopulation. (F) Telomerase activity was detected by TeloTAGGG telomerase PCR enzyme-linked immunosorbent assay (ELISA (Roche). "+" was regarded as telomerase positive (absorbance [$\Delta$A] is greater than 0.2 $A_{450nm}$-$A_{690nm}$ units). PC, positive control; NC, negative control. Values are expressed as mean $\pm$ SD.

of serial transplantation or from 18-month-old mice (Fig. 6B) were transplanted into 8-week-old $Fah^{-/-}$ recipients. Mitotic structures with multipolar spindles or tripolar division were detected during hepatocyte proliferation *in vivo* (Fig. 6C). Analysis of liver sections using fluorescence imaging technology revealed the existence of ploidy reversal, reflected by a reduction in DNA content (Fig. 6D). Furthermore, pure diploid hepatocytes shown in samples of the above two mice groups produced daughter cells with 4c and 8c DNA content. Tetraploid and octoploid donor hepatocytes also showed similar ploidy redistribution (Fig. 6E,F). In addition, ploidy plasticity was also found in the *in vitro* cultured primary hepatocytes that were detected initially as diploid, tetraploid, or octoploid. Polyploid hepatocytes from 18-month-old mice showed a lower proliferation capacity compared to diploid hepatocytes from the same mice, and compared to the hepatocytes with all three ploidies from mice of the 12th round of serial transplantation (Fig. S4).

Together, the ratio of polyploidy among hepatocytes increased with liver aging, reversed to the youthful distribution upon transplantation of aged hepatocytes, and remained stable over time when there was continuous repopulation of hepatocytes.

***Human Hepatocytes Undergo Senescence With Age and Become Rejuvenated After Cell Transplantation.*** Similar to mouse hepatocytes, human hepatocytes gradually become senescent with age.[2] We examined healthy liver tissue from humans and found that the cell size of human hepatocytes from 55- to 65-year-olds was much larger than those of 21- to 30-year-olds (Fig. 7A). On staining liver sections we found that the proportion of SA-$\beta$-gal-positive and $\gamma$-H2A.X-positive hepatocytes was $68.9 \pm 2.69\%$ and $71.8 \pm 5.07\%$, respectively, in the liver of older persons, but only $8.2 \pm 1.87\%$ and $8.6 \pm 1.61\%$ in younger liver (Fig. 7B; S5A,B). Analysis of the DNA content of human hepatocytes revealed that the percentage of polyploid cells increased from $8.8 \pm 1.1\%$ in 21- to 30-year-olds to $32.6 \pm 0.9\%$ in 55- to 65-year-olds (Fig. S5C,D). Moreover, the percentages of SA-$\beta$-gal and $\gamma$-H2A.X-positive cells among polyploid hepatocytes were significantly higher than it was for diploid cells in older volunteers, suggesting that polyploid hepatocytes in older humans, like in mice, are more prone to senescence (Fig. 7C,D).

To further investigate whether human senescent hepatocytes could rejuvenate to regain proliferation capacity, young (21-30 years) and old (55-65 years) human hepatocytes were isolated and xenotransplanted into 8-week-old $Fah^{-/-}Rag2^{-/-}$ mice. At 10 weeks posttransplantation, human hepatocytes could be identified by staining with an antibody specific to human albumin (Alb) in mouse recipients, and there was no significant difference in the percentage of liver repopulation between old and young human hepatocytes (Fig. 7E; S5E,F). As shown in Fig. 7E, $\gamma$-H2A.X-positive staining was seen mainly in the host mouse hepatocytes surrounding Alb-positive human cells, and only

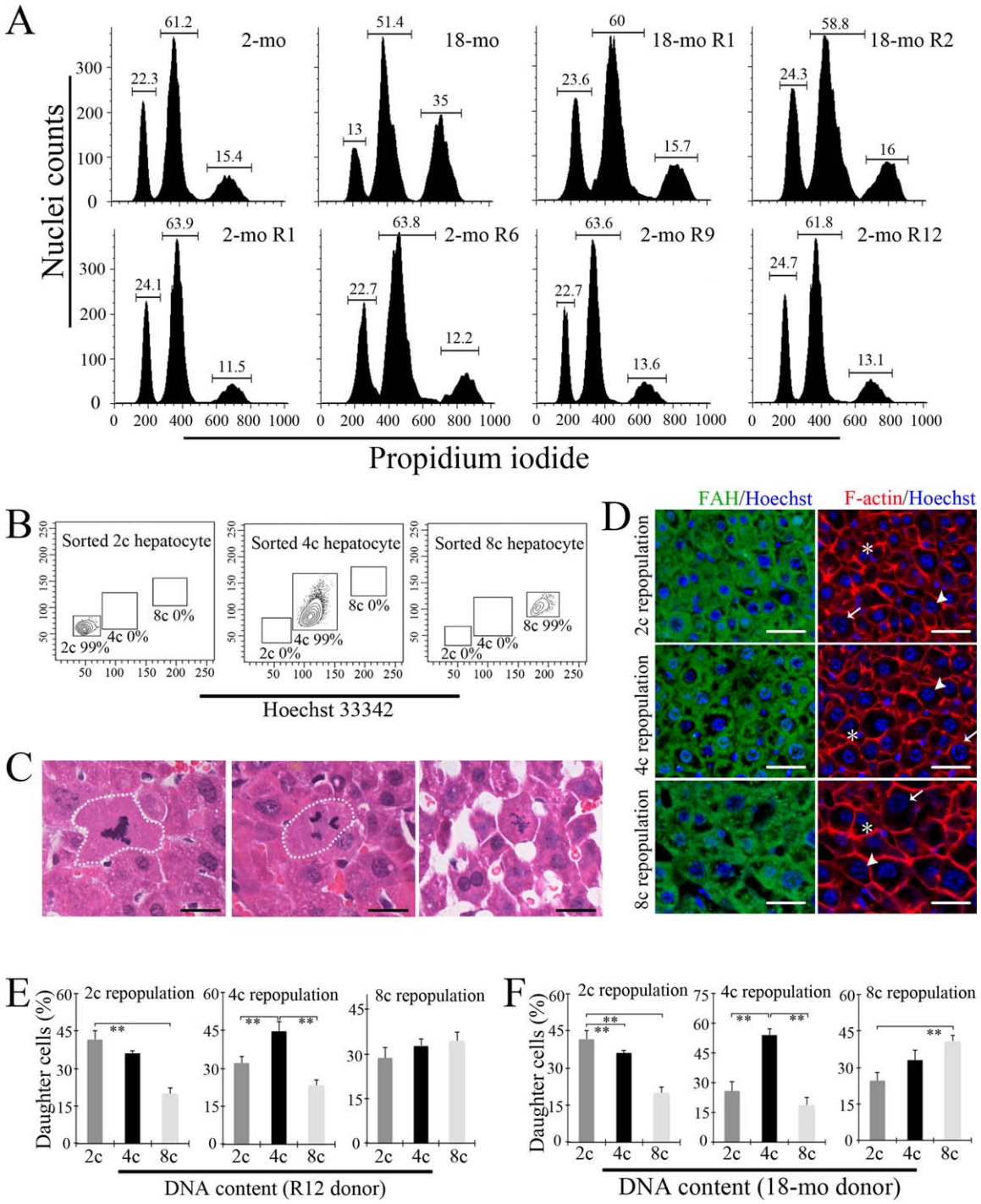


Fig. 6. Ploidy conversion after hepatocyte transplantation. (A) Flow cytometry histogram showing the percentages of diploid, tetraploid, and octoploid hepatocytes in 2-month-old, 18-month-old mice, hepatocytes from recipients 2 months after primary (R1) or secondary (R2) transplantation of 18-month-old hepatocytes and hepatocytes from recipients 2 months after the 1st, 6th, 9th, 12th transplantation of 2-month-old hepatocytes. (B) Representative images of the FACS analysis and sorting of highly pure 2c, 4c, and 8c hepatocytes from 12 rounds serially transplanted hepatocytes using Hoechst 33342 staining. (C) Hematoxylin and eosin (H&E) staining of liver sections demonstrating atypical mitosis, such as tripolar spindles (left), tripolar division (middle), and multipolar spindles (right), representing ploidy conversion in repopulating hepatocytes. (D) Immunofluorescence staining for FAH, F-actin, and Hoechst 33342 in liver sections after transplantation of 2c, 4c, and 8c hepatocytes. Asterisks mark diploid hepatocytes, arrowheads marks tetraploid hepatocytes, and arrows mark octaploid hepatocytes. (E,F) Ploidy distribution ratio in the daughter cells after liver repopulation by 12 rounds serially transplanted hepatocytes (E) and 18-month-old hepatocytes (F) by FACS analysis. $^{**}P < 0.01$; Scale bars = 20 $\mu$m.

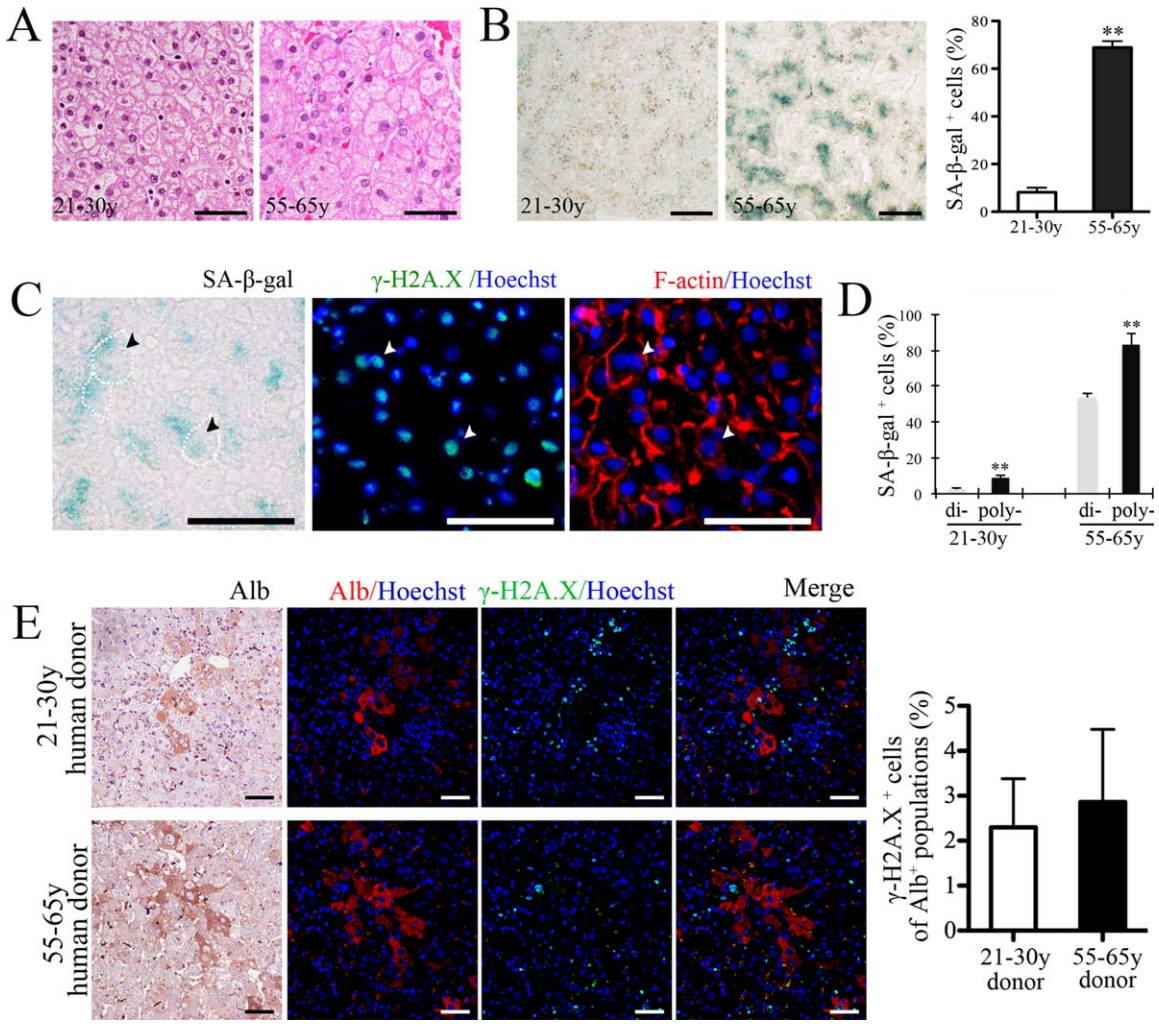


Fig. 7. Senescent human hepatocytes can repopulate the FAH$^{-/-}$ mouse liver. (A) H&E staining of human liver samples from 21- to 30-year-olds (young) and 55- to 65-year-olds (old). Enlarged hepatocytes are observed in human liver from older adults compared to younger adult liver. (B) Representative images of young and old human liver sections stained for SA-$\beta$-gal activity. On quantification of SA-$\beta$-gal-positive hepatocytes (right panel), they were found to be significantly more prevalent in older liver tissue than that in younger liver. $^{**}P < 0.01$ versus young human hepatocytes. (C) Histochemical analysis of older human liver tissue sections stained for SA-$\beta$-gal, $\gamma$-H2A.X, F-actin, and Hoechst. The left panel shows SA-$\beta$-gal staining. The middle is expression of $\gamma$-H2A.X. The right shows the DNA content per cell. The white dashed line and arrowhead mark representative senescent cells. (D) The percentage of SA-$\beta$-gal-positive cells in diploid and polyploid hepatocytes from young and old human liver. $^{**}P < 0.01$ versus diploid hepatocytes. (E) Immunohistochemistry and immunofluorescence staining with a human-specific Alb antibody, $\gamma$-H2A.X and Hoechst of mouse tissue repopulated with young (top) and old (bottom) human donor cells. The bar graph on the right shows the percentage of $\gamma$-H2A.X-positive cells in repopulated Alb-positive human cells. Shows are mean $\pm$ SD. Scale bars = 50 $\mu$m.

about 5% of the human hepatocytes stained positive for $\gamma$-H2A.X, much less than the more than 70% that was seen within the donor human tissue with human hepatocytes before transplantation. These results confirmed that human senescent hepatocytes could become rejuvenated to recover proliferation capacity after reentry into the cell cycle, as is the case for mice.

## Discussion

Understanding the mechanism of liver aging has special significance for the treatment of liver diseases that are influenced by age.[33,34] Mature hepatocytes are generally quiescent, but are poised to enter into the cell cycle immediately upon injury, a property that is rare among diverse differentiated cell types *in vivo*. Until now, it was not clear whether there was a limit to the proliferation capacity of hepatocytes. Our data indicate that repopulating hepatocytes could divide at least 130 times during 12 rounds of transplantation, which breaks the traditional concept of noncancerous cells having a limited proliferation capacity. More interestingly, we demonstrated that the aged hepatocytes were able to rejuvenate and take on full

proliferative capacity after transplantation. This study suggests that old hepatocytes could still be considered for cell therapy treatment of liver diseases. It also supplies a basis for strategies to the delay or reverse hepatocytes senescence for clinical applications.

Previously published competitive experiments with naive hepatocytes and serially repopulated hepatocytes demonstrated that serial transplantation neither enhances nor diminishes the repopulation capacity of these cells.[35] It has been reported that diploid and octoploid hepatocytes of 8-week-old mice proliferated equivalently *in vivo*.[24,36] Here, we extended the research to present the kinetics of liver repopulation for hepatocytes from various donor ages and ploidy levels. Our results indicate that young, 2-month-old hepatocytes (either diploid, or tetraploid, or octoploid) had the same repopulation capacity as "old" hepatocytes that had undergone 12 rounds of serial repopulations in $Fah^{-/-}$ mice. Our results also indicate that 18-month-old, predominantly senescent hepatocytes appear to have an equivalent rate of engraftment in the liver, but had a slower initial rate of proliferation compared to the 2-month-old hepatocytes. However, they could repopulate the liver to the same degree, and on subsequent transplantation they were equivalent to younger hepatocytes. Our studies indicate that serial transplantation in $Fah^{-/-}$ mice is an ideal method to study hepatocyte senescence. Shown in a previous study of serial transplantations in $Fah^{-/-}$ mice,[18] it is unlikely that there is selection of a special group of hepatocytes during serial repopulation. Therefore, our findings on hepatocyte senescence during serial repopulation document the complete panels of hepatocytes in whole liver.

Hepatocyte polyploidy was considered an age-dependent process, although it appears in late fetal development and postnatal maturation.[1,37] However, the biological significance of polyploidy in the liver, as well as the relationship between hepatocyte polyploidy and senescence, were not fully elucidated. In this study we documented that senescence was rare among octoploid hepatocytes in young mice, as well as in diploid and tetraploid hepatocytes. However, the percentage of senescent, octoploid hepatocytes increased with age and a majority of aged octoploid hepatocytes expressed cell senescence markers. More interestingly, polyploid hepatocytes can produce diploid, tetraploid, and octoploid daughter hepatocytes after cell transplantation, a phenomenon that has been called "ploidy conveyor."[24] Our results support the notion that ploidy conversion may be conserved in hepatocytes, as the proportions of polyploid cells remained stable during serial transplantation, and the percentage of octoploid hepatocytes decreased after transplantation of 18-month-old hepatocytes transplantation. These findings also implicate the ploidy conveyor in the reversal of hepatocyte senescence. In addition, we showed similar results for human hepatocytes. Senescent human hepatocytes rejuvenated to restore proliferative capacity after xenotransplantation, a finding of great significance for future studies on liver diseases and liver cell therapy.

In the absence of telomerase activity in cells, telomere length decreases with each cell cycle until it reaches a critical length limit, which leads to cell senescence. However, studies on normal human livers over a wide age range (5-79 years) indicate that hepatocytes and cholangiocytes maintain a constant telomere length with age.[19] We found similar results for mouse hepatocytes. Generally, telomerase activity is absent in differentiated, mature cells, but exists in stem cells and cancer cells, and promote the proliferation capacity of hematopoietic stem cells during serial transplantations.[38] Similarly, our data suggested that the telomerase activity dissipates in aged liver but reactivates with serial transplantations. It is possible that reactivation of telomerase activity enables inhibition or reversal of the senescence program in repopulating hepatocytes.

In this study we confirmed that aged hepatocytes accumulate senescence markers such as DNA damage markers and $p16^{ink4a}$ and p21, but do not undergo telomere shortening. It is possible that a common pathway for cell cycle regulation leads to arrest by way of p53 and p21, in which CDK2, CDK4, and CDK6 maintain Rb-family proteins in a hypo-phosphorylated state, promoting binding of E2F to effect a $G_1$ cell-cycle arrest, halting cellular proliferation. The precise molecular mechanism leading to hepatocyte senescence and its reversal is the subject of further study.

## References

1. Gupta S. Hepatic polyploidy and liver growth control. Semin Cancer Biol 2000;10:161-171.
2. Hoare M, Das T, Alexander G. Ageing, telomeres, senescence, and liver injury. J Hepatol 2010;53:950-961.
3. Zhang C, Cuervo AM. Restoration of chaperone-mediated autophagy in aging liver improves cellular maintenance and hepatic function. Nat Med 2008;14:959-965.
4. Collado M, Blasco MA, Serrano M. Cellular senescence in cancer and aging. Cell 2007;130:223-233.
5. Campisi J. Senescent cells, tumor suppression, and organismal aging: good citizens, bad neighbors. Cell 2005;120:513-522.
6. Hayflick L. The limited in vitro lifetime of human diploid cell strains. Exp Cell Res 1965;37:614-636.
7. Von Figura G, Hartmann D, Song Z, Rudolph KL. Role of telomere dysfunction in aging and its detection by biomarkers. J Mol Med (Berl) 2009;87:1165-1171.
8. Krishnamurthy J, Torrice C, Ramsey MR, Kovalev GI, Al-Regaiey K, Su L, et al. Ink4a/Arf expression is a biomarker of aging. J Clin Invest 2004;114:1299-1307.

9. Kim WY, Sharpless NE. The regulation of INK4/ARF in cancer and aging. Cell 2006;127:265-275.
10. Kuilman T, Michaloglou C, Mooi WJ, Peeper DS. The essence of senescence. Genes Dev 2010;24:2463-2479.
11. Wang C, Jurk D, Maddick M, Nelson G, Martin-Ruiz C, Von Zglinicki T. DNA damage response and cellular senescence in tissues of aging mice. Aging Cell 2009;8:311-323.
12. Beauséjour CM, Krtolica A, Galimi F, Narita M, Lowe SW, Yaswen P, et al. Reversal of human cellular senescence: roles of the p53 and p16 pathways. EMBO J 2003;22:4212-4222.
13. Menthena A, Koehler CI, Sandhu JS, Yovchev MI, Hurston E, Shafritz DA, et al. Activin A, p15INK4b signaling, and cell competition promote stem/progenitor cell repopulation of livers in aging rats. Gastroenterology 2011;140:1009-1020.
14. Kuilman T, Michaloglou C, Vredeveld LC, Douma S, van Doorn R, Desmet CJ, et al. Oncogene-induced senescence relayed by an interleukin-dependent inflammatory network. Cell 2008;133:1019-1031.
15. Stepanova L, Sorrentino BP. A limited role for p16Ink4a and p19Arf in the loss of hematopoietic stem cells during proliferative stress. Blood 2005;106:827-832.
16. Lapasset L, Milhavet O, Prieur A, Besnard E, Babled A, Ait-Hamou N, et al. Rejuvenating senescent and centenarian human cells by reprogramming through the pluripotent state. Genes Dev 2011;25:2248-2253.
17. Conboy IM, Conboy MJ, Wagers AJ, Girma ER, Weissman IL, Rando TA. Rejuvenation of aged progenitor cells by exposure to a young systemic environment. Nature 2005;433:760-764.
18. Overturf K, Al-Dhalimy M, Ou C-N, Finegold M, Grompe M. Serial transplantation reveals the stem-cell-like regenerative potential of adult mouse hepatocytes. Am J Pathol 1997;151:1273-1280.
19. Verma S, Tachtatzis P, Penrhyn-Lowe S, Scarpini C, Jurk D, Von Zglinicki T, et al. Sustained telomere length in hepatocytes and cholangiocytes with increasing age in normal liver. HEPATOLOGY 2012;56:1510-1520.
20. Liu L, Yannam GR, Nishikawa T, Yamamoto T, Basma H, Ito R, et al. The microenvironment in hepatocyte regeneration and function in rats with advanced cirrhosis. HEPATOLOGY 2012;55:1529-1539.
21. Guidotti JE, Bregerie O, Robert A, Debey P, Brechot C, Desdouets C. Liver cell polyploidization: a pivotal role for binuclear hepatocytes. J Biol Chem 2003;278:19095-19101.
22. Celton-Morizur S, Merlen G, Couton D, Desdouets C. Polyploidy and liver proliferation: central role of insulin signaling. Cell Cycle 2010;9:460-466.
23. Celton-Morizur S, Merlen G, Couton D, Margall-Ducos G, Desdouets C. The insulin/Akt pathway controls a specific cell division program that leads to generation of binucleated tetraploid liver cells in rodents. J Clin Invest 2009;119:1880-1887.
24. Duncan AW, Taylor MH, Hickey RD, Hanlon Newell AE, Lenzi ML, Olson SB, et al. The ploidy conveyor of mature hepatocytes as a source of genetic variation. Nature 2010;467:707-710.
25. Duncan AW, Newell AEH, Bi W, Finegold MJ, Olson SB, Beaudet AL, et al. Aneuploidy as a mechanism for stress-induced liver adaptation. J Clin Invest 2012;122:3307-3315.
26. Wang X, Foster M, Al-Dhalimy M, Lagasse E, Finegold M, Grompe M. The origin and liver repopulating capacity of murine oval cells. Proc Natl Acad Sci U S A 2003;100(Suppl 1):11881-11888.
27. He Z, Zhang H, Zhang X, Xie D, Chen Y, Wangensteen KJ, et al. Liver xeno-repopulation with human hepatocytes in Fah−/−Rag2−/− mice after pharmacological immunosuppression. Am J Pathol 2010;177:1311-1319.
28. Li F, Liu P, Liu C, Xiang D, Deng L, Li W, et al. Hepatoblast-like progenitor cells derived from embryonic stem cells can repopulate livers of mice. Gastroenterology 2010;139:2158-2169.
29. Yu B, He Z, You P, Han Q, Xiang D, Chen F, et al. Reprogramming fibroblasts into bipotential hepatic stem cells by defined factors. Cell Stem Cell 2013;13:328-340.
30. Huang P, He Z, Ji S, Sun H, Xiang D, Liu C, et al. Induction of functional hepatocyte-like cells from mouse fibroblasts by defined factors. Nature 2011;475:386-389.
31. Stuart GR, Glickman BW. Through a glass, darkly: reflections of mutation from lacI transgenic mice. Genetics 2000;155:1359-1367.
32. Toyoda H, Bregerie O, Vallet A, Nalpas B, Pivert G, Brechot C, et al. Changes to hepatocyte ploidy and binuclearity profiles during human chronic viral hepatitis. Gut 2005;54:297-302.
33. Al-Chalabi T, Boccato S, Portmann BC, McFarlane IG, Heneghan MA. Autoimmune hepatitis (AIH) in the elderly: a systematic retrospective analysis of a large group of consecutive patients with definite AIH followed at a tertiary referral centre. J Hepatol 2006;45:575-583.
34. Czaja AJ, Carpenter HA. Distinctive clinical phenotype and treatment outcome of type 1 autoimmune hepatitis in the elderly. HEPATOLOGY 2006;43:532-538.
35. Overturf K, Al-Dhalimy M, Finegold M, Grompe M. The repopulation potential of hepatocyte populations differing in size and prior mitotic expansion. Am J Pathol 1999;155:2135-2143.
36. Weglarz TC, Degen JL, Sandgren EP. Hepatocyte transplantation into diseased mouse liver kinetics of parenchymal repopulation and identification of the proliferative capacity of tetraploid and octaploid hepatocytes. Am J Pathol 2000 157;1963-1974.
37. Turner R, Lozoya O, Wang Y, Cardinale V, Gaudio E, Alpini G, et al. Human hepatic stem cell and maturational liver lineage biology. HEPATOLOGY 2011;53:1035-1045.
38. Allsopp RC, Morin GB, DePinho R, Harley CB, Weissman IL. Telomerase is required to slow telomere shortening and extend replicative lifespan of HSCs during serial transplantation. Blood 2003;102:517-520.

## Supporting Information

Additional Supporting Information may be found in the online version of this article at the publisher's website.

**Supporting material**

## Additional methods

**Mice:** All experiments were performed with congenic mice with the 129S4 background. 129S4 wild-type mice (2-, 6-, 12- and 18-months-old), $Fah^{-/-}$ and $Fah^{-/-}Rag\text{-}2^{-/-}$ mice (8-months-old) (1), and Rosa26R-LacZ transgenic mice (2- and 18-months-old) were housed in temperature- and light-dark cycle-controlled rooms. $Fah^{-/-}$ and $Fah^{-/-}Rag\text{-}2^{-/-}$ mice were maintained with 7.5 mg/L 2-(2-nitro-4-trifluoromethylbenzoyl)-1, 3-cyclohexanedione (NTBC) in the drinking water. All mice received humane care according to the guidelines of Second Military Medical University Animal Care and Use Committees.

**Liver perfusion and hepatocyte isolation:** Livers from the 129S4 wild-type male mice and the Rosa26R-LacZ transgenic mice were perfused with 0.5 mg/ml collagenase D (Roche, Indianapolis, IN) through the portal vein. The dissociated cells were passed through a 70 μm cell strainer (BD Biosciences, San Jose, CA) to remove clumps. Cells were centrifuged at 50 g for 2 min twice to pellet down hepatocytes and the supernatant was removed. The viability of cell was at least 85% as evaluated by Trypan blue (Sigma-Aldrich, St. Louis, MO) exclusion.

Human liver tissues were provided by Eastern Hepatobiliary Surgery Hospital, Second Military Medical University (Shanghai, China), which were from normal liver tissues adjacent to hepatic hemangioma after a surgical resection. All human tissues were negative for HBV infection. Patients' characteristics and clinical features are listed in supplemental table 1. Each patient gave written, informed consent. Experiments were approved by Ethical Committee on Ethics of Biomedicine Research, Second Military Medical University.

**Quantitation of nodule areas from donor repopulation:** Fah-stained liver surface areas were analyzed by Image-Pro software (Media Cybernetics, Silver Spring, MD) according to previous report (2). The nodule areas were determined under low-power magnification by measuring the major axes (a, b), and the formula $A=\pi[1/4(a+b)]^2$ was used to calculating the areas.

**Analysis and isolation by Flow Cytometry:** To quantify ploidy by flow cytometry, hepatocytes from 2-, 6-, 12-, 18-month-old mice and serially transplanted mice were fixed in ice-cold 75% (vol/vol) ethanol (Sinoreagent, Shanghai, CHN) and stained with 50 μg/mL propidium iodide (Sigma-Aldrich, St. Louis, MO) in phosphate-buffered saline supplemented with 1 μg/mL (wt/vol) RNAse A (Sigma-Aldrich, St. Louis, MO). DNA content of a minimum of 30,000 nuclei per liver sample was analyzed by a FACS-Calibur flow cytometer (BD Biosctoences, San Jose, CA).

For isolation of hepatocyte with different ploidy, hepatocytes were incubated with 15 μg/ml Hoechst 33342 (Sigma-Aldrich, St. Louis, MO) for 30 min at 37 °C. Cells were sorted with InFlux flow cytometer (Beckton Dickinson Franklin Lakes, NJ) using a 150 μm nozzle. Dead cells were excluded on the basis of 5 μg/ml propidium iodide (Sigma-Aldrich, St. Louis, MO). Populations of different ploidies were identified with parameter of DNA content using a 355-nm laser and 425-440-nm bandpass filter. Sorted hepatocytes were collected in DMEM (Thermo Scientific, Waltham, MA) containing 50% fetal bovine serum (Thermo Scientific, Waltham, MA). The purity of sorted populations was determined at the end of each sorting and highly purified populations were used for further experiments.

The β-gal positive hepatocytes were detected and sorted by using FluoReporter lacZ Flow Cytometry Kit (Invitrogen, Carlsbad, CA) as following the manufacture's instructions.

***In situ* detection of ploidy:** Microscopic analysis after F-actin and Hoechst 33342 stainings was used to determine the ploidies of both mononucleated and binucleated hepatocytes (3, 4). As done previously, freshly liver tissues were embedded into optimum cutting temperature compound (Sakura Finetek, Torrance, CA). Frozen sections were cut into 4 μm sections and fixed with 4%

paraformaldehyde. F-actin were labeled with Alexa Fluor® 568 Phalloidin (1:400, Invitrigen, Carlsbad, CA) to identify the outline of a cell, incubated for 30min at room temperature. Hoechst 33342 (0.2ug/ml) was used to stain and quantify DNA in each nucleus. Image analysis was performed in 12 bits using IPLab Spectrum software. To measure the size of the nuclei and cells, we selected only nuclei or cells with clear margins. A minimum of 300 hepatocytes were analyzed and counted from eight to twelve separate fields per sample.

**SA-β-Gal Activity:** As previously described (5, 6, 7), tissues were excised and embedded into optimum cutting temperature compound (Sakura Finetek, Torrance, CA). Frozen sections were cut into 4 μm sections and fixed with fixative solution (PBS containing 4% paraformaldehyde, 2% glutaraldehyde, 5 mM EGTA, and 2 mM MgCl2) for 10 min, then were incubated in fresh senescence-associated β-Gal (SA-β-Gal) stain solution at 37°C (no $C0_2$) using a β-gal staining kit (Invitrogen, Carlsbad, CA). Staining was evident in 2-4 hr and was maximal at 12-16 hr.

**Immunohistochemistry (IHC) and Immunocytochemistry (ICC):** For immunohistochemistry staining, fresh liver pieces were fixed in 4% paraformaldehyde, embedded in paraffin, and sectioned into 2 μm-thick slices. The sections were deparaffinized, rehydrated, and heated in a pressure cooker for 3 min at 121°C/100 kpa in citrate buffer (pH 6.0). Incubation with

primary antibodies was done at 4 °C overnight and with secondary antibodies conjugated with fluorescent dye or HRP at 37 °C for 30 min. DAB (Vector Laboratories, Burlingame, CA) staining was applied on the sections and incubated with HRP-conjugated antibody until an adequate intensity was achieved. The sections were counterstained in hematoxylin (Sigma-Aldrich, St. Louis, MO) and covered in neutral balsam (Solarbio, Beijing, CHN) after dehydration in ethanol and xylene (all from Sinoreagent, Shanghai, CHN). For immunocytochemical staining, cells were fixed with PBS containing 4% paraformaldehyde for 20 min, permeabilized and blocked with blocking buffer (PBS containing 0.1% Triton X-100, 1% BSA, and 10% normal goat serum) for 30 minutes. Cells were then incubated with rabbit anti-mouse H2A primary antibody at 4 °C overnight, followed by fluorescence-tagged secondary antibodies at 37 °C for 30 min. Nuclei were stained with 4', 6-diamidino-2-phenylindole (DAPI) (Sigma-Aldrich, St. Louis, MO). Images were acquired with a 50i Nikon fluorescence microscope (Nikon, Melville, NY). The list of primary and secondary antibodies is reported in Table. Images were processed with Adobe Photoshop CS4 software (San Jose, CA).

**Primary hepatocyte culture and analysis of cell proliferation:** Hepatocytes collected by liver perfusion or after FACS were seeded on collagen-coated 6-well plates. Cells were initially cultured in DMEM with 4.5 $gl^{-1}$ glucose (Thermo Scientific, Waltham, MA), 10% FBS (Thermo Scientific, Waltham,

MA), non-essential amino acids (Invitrogen, Carlsbad, CA) and antibiotic-antimycotic (Invitrogen, Carlsbad, CA). After 24h, the culture medium was replaced with SUM3 medium with 0.5% FBS as described. For the proliferation assay, cells were incubated for 12h with BrdU labeling regent (final concentration 100uM) (Sigma-Aldrich, St. Louis, MO). For BrdU staining, cells were fixed with a 1:1 mixture of ice-cold methanol: glacial acetic acid after washing with PBS, and then incubated with 2N HCL for 30 min at room temperature. Then cells were incubated with primary and second antibody as with the IHC protocols.

**RNA isolation, RT-PCR and quantitative PCR:** Total RNA from cells was isolated with Trizol reagent (Invitrogen, Carlsbad, CA) according to the manufacturer's instructions. All reverse-transcriptase reactions were carried out with SuperScript II reverse transcriptase (Invitrogen, Carlsbad, CA) according to the manufacturer's protocol. Mouse specific primers including p16, p21, and p53 were designed by Primer Premier 5. Quantitative PCR was performed in three repeats of each sample with ABI-7900 (Applied Biosystems, Foster, City, CA) by SYBR Green master mix (Applied Biosystems, Foster, City, CA). Fold change was calculated by the $2\text{-}\Delta\Delta_{CT}$ method (8).

**Protein Isolation and Western Blot:** Western-blot analysis was performed as described previously (9). 50 μg liver total proteins were extracted from mouse

liver tissues using Minute$^{TM}$ Total Protein Extraction Kit (Invent Biotechnologies, Eden Prairie, MN) according to manufacturer's instructions. The protein was loaded into acrylamide gels, and transferred onto a PVDF membrane (Millipore, Temecula, CA). Membranes were blocked with blotto (5% nonfat milk powder in PBS plus 0.1% Tween 20) for 1 hr at room temperature and then incubated with primary antibodies at 4 °C overnight. Membranes were washed three times with PBS plus 0.1% Tween 20 and incubated with appropriate secondary antibody conjugated with HRP. Protein bands were detected by chemiluminescent substrate (Thermo Scientific, Waltham, MA). The list of primary and secondary antibodies is summarized as below.

**Primary antibodies used in the IHC and western blot assay**

| Primary Antibody | Brand | Cat. No. |
|---|---|---|
| γ-H2AX (phosphor S139) | Epitomics | 2212-1 |
| P16 (F-4) | Santa Cruz | sc-74401 |
| P21 (F-5) | Santa Cruz | sc-6246 |
| P53 | Abcam | ab26 |
| Fah | HepatoScience | HS602-910 |
| CDK2 (M2) | Santa Cruz | sc-163 |
| CDK4 (c-22) | Santa Cruz | sc-260 |
| p-Rb (ser807/811) | Cell Signaling | 9308 |
| Alpha tubulin | Abcam | ab15246 |
| Alexa Fluor® 568 Phalloidin | Invitrogen | A12380 |

| | | |
|---|---|---|
| TERT (D-16) | Santa Cruz | sc-68720 |
| Albumin | EnoGene | E2200340 |
| BrdU | Abcam | ab6326 |
| Hnf4a | Santa Cruz | sc-8987 |

**Telomerase activity and telomere length assay:** Quantification of telomerase activity was performed with a telomerase PCR ELISA kit (Roche, Indianapolis, IN). Telomere length was determined by QPCR using the modified Cawthon's method (10). Genomic DNA was extracted from isolated mouse hepatocytes using the DNeasy Blood & Tissue Kit (QIAGEN, Valencia CA) according to the manufacturer's instructions. Briefly, telomere and single copy gene PCRs were performed in separate 96-well plates using the same DNA sample. The telomere/single copy gene (T/S) ratio was calculated as the index of telomere length in each sample. Triplicate PCR reactions for each sample were performed with Power SYBR Green PCR Master Mix (Applied Biosystems, Foster City, CA), DNA and primer pairs using the ABI 7900 real time PCR System. Primers for telomeres and the single copy gene 36B4 were added to final concentrations of 0.2 μM and 0.3 μM, respectively. PCR was performed at 95°C for 10 min, followed by 30 cycles of 95 °C for 5 s, 58 °C for 10s, and 72 °C for 40 s for the 36B4 reaction, or 40 cycles of 95 °C for 5 s, 56 °C for 10 s, and 72 °C for 60 s for the telomere reaction. Standard curves for both telomere length and the single copy gene were generated from five concentrations (42, 25.2, 15.1, 9.1, 5.4 ng/aliquot) of a reference DNA sample

serially diluted 1.68 fold with PCR grade water.

**Statistical analysis**: Data were subjected to Student's t-test. $p < 0.05$ was considered statistically significant. Data are presented as mean ± standard deviation (s.d.).

## References

1. Overturf K, Al-Dhalimy M, Tanguay R, Brantly M, Ou C-N, Finegold M, Grompe M. Hepatocytes corrected by gene therapy are selected in vivo in a murine model of hereditary tyrosinaemia type I. Nature genetics 1996;12: 266-273.
2. Weglarz TC, Degen JL, Sandgren EP. Hepatocyte Transplantation into Diseased Mouse Liver Kinetics of Parenchymal Repopulation and Identification of the Proliferative Capacity of Tetraploid and Octaploid Hepatocytes. Am J Pathol 2000 157;1963-1974.
3. Guidotti JE, Bregerie O, Robert A, Debey P, Brechot C, Desdouets C. Liver cell polyploidization: a pivotal role for binuclear hepatocytes. J Biol Chem 2003;278:19095-19101.
4. Toyoda H, Bregerie O, Vallet A, et al. Changes to hepatocyte ploidy and binuclearity profiles during human chronic viral hepatitis. Gut 2005;54:297–302.
5. Lee BY, Han JA, Im JS, Morrone A, Johung K, Goodwin EC, Kleijer WJ, et al. Senescence-associated β-galactosidase is lysosomal β-galactosidase. Aging Cell 2006;5:187-195.
6. Debacq-Chainiaux F, Erusalimsky JD, Campisi J, Toussaint O. Protocols to detect senescence-associated beta-galactosidase (SA-beta-gal) activity, a biomarker of senescent cells in culture and in vivo. Nat Protoc 2009;4: 1798-1806.

7. Dimri GP, Lee X, Basile G, Acosta M, Scott G, Roskelley C, Medrano EE, et al. A biomarker that identifies senescent human cells in culture and in aging skin in vivo. Proc Natl Acad Sci U S A 1995;92:9363-9367.
8. Schmittgen TD, Livak KJ. Analyzing real-time PCR data by the comparative CT method. Nature Protocols 2008;3:1101-1108.
9. Wangensteen KJ, Wilber A, Keng VW, He Z, Matise I, Wangensteen L, Carson CM, et al. A facile method for somatic, lifelong manipulation of multiple genes in the mouse liver. Hepatology 2008;47:1714-1724.
10. Cawthon RM. Telomere measurement by quantitative PCR. Nucleic acids research 2002;30:47-47.

Supplemental table 1

Clinical characteristics of patients

| Patient number | Sex | Age (year) | Type of disease | TB (mg/dL) | ALT (U/L) | AST (U/L) | HBV/ HCV | AFP (ug/L) |
|---|---|---|---|---|---|---|---|---|
| 1 | M | 28 | Hemangioma | 0.39 | 24 | 21 | N/N | 6.5 |
| 2 | M | 24 | Hemangioma | 0.91 | 10 | 18 | N/N | 2.2 |
| 3 | F | 28 | Hemangioma | 0.41 | 9 | 15 | N/N | 1.2 |
| 4 | M | 65 | Hemangioma | 0.94 | 17 | 25 | N/N | 1.9 |
| 5 | M | 60 | Hemangioma | 0.82 | 6 | 13 | N/N | 2.7 |
| 6 | M | 63 | Hemangioma | 0.46 | 16 | 13 | N/N | 2.2 |

M: male; F: female; TB: total bilirubin; ALT: alanine aminotransferase; AST: aspartate aminotransferase；HBV: hepatitis B virus; HCV: hepatitis C virus; N: negative; AFP: alpha-fetoprotein.

## Supplementary figure

**Supplementary figure 1. Hepatocyte senescence increases with age.**

(A) H&E staining of liver samples from 2-, 6-, 12- and 18-month-old mice. (B) Percentage of SA-β-gal positive cells in the livers at the indicated stages. Values shown are means ± S.D. $^{**}p < 0.01$. (C) Expression of γ-H2A.X was detected and analyzed in the livers of 2-, 6-, 12- and 18-month-old mice by histochemical staining. Values shown are means ± S.D. $^{**}p < 0.01$. (D) Expression of p16 and p21 in the livers of four indicated groups was analyzed by Western blot. Protein expression in 2-month-old mouse livers was taken as the baseline and considered equal to 1. $^{**}p < 0.01$ versus the 2-month-mice. (E) Bright field image of primary hepatocytes from 2- and 18-month-old mice 2 days after culture. Cells with blue perinuclear staining were SA-β-gal positive cells. Box: a magnification. In right panel values shown are means ± S.D. $^{**}p < 0.01$ versus the 2-month-old hepatocytes. (F) Proliferating hepatocytes from 2- and 18-month-old mice as indicated by immunohistochemistry staining of Hnf4a, BrdU and Hoechst after 3 days culture. Arrows indicate the hepatocytes in S phase. The percentage of BrdU-positive cells at different days after plating are presented as mean ± S.D. $^{**}p < 0.01$ versus the 2-month-old hepatocytes. Scale bar, 100 μm.

**Supplementary figure 2. Evaluation of hepatic polyploidization and cellular senescence.**

(A) Distribution of hepatic ploidy populations in the livers of 2-, 6-, 12- and 18-month-old mice by FACS analysis. 2c, 4c, and 8c hepatocyte represent diploid, tetraploid and octaploid hepatocytes, respectively. (B) mRNA expressions of p16, p21, and p53 among three ploidy isolated from 2- and 18-month-old mice were compared using quantitative real-time PCR. (C) The percentages of γ-H2A.X positive cells in isolated diploid, tetralpoid and octaploid hepatocytes were counted by immunocytochemistry staining. Arrowhead indicated the γ-H2A.X positive cells. *, $p < 0.05$; **, $p < 0.01$; Scale bar, 50 μm.

**Supplementary figure 3. Three populations of hepatocytes from 2-month-old livers have the same capacity for engraftment and proliferation.**

(A-D) Comparison of the capacity of engraftment and repopulation from 2c, 4c and 8c hepatocytes isolated from 2-month-old mice at 2 (A), 5 (B), 8 (C), and 10 (D) weeks post-transplantation. 2c, 4c and 8c represent diploid, tetraploid and octoploid hepatocytes respectively. (E) The percentages of liver repopulation of 2c, 4c and 8c donor hepatocytes after 2, 5, 8, 10 weeks later. Values shown are means ± S.D. Scale bar, 200 μm.

**Supplementary figure 4. Polyploid hepatocytes proliferate and undergo ploidy reversal *in vitro.***

(A) S-phase fraction in cultured 2c, 4c and 8c hepatocytes from R12 and 18 months liver as indicated by BrdU labeling. Red cells represent proliferating hepatocytes. (B, C) The percentages of BrdU positive cells in R12 repopulated hepatocytes (B) and 18 months hepatocytes (C). Values shown are means ± S.D. (D) Highly pure (99%) 2c, 4c, and 8c hepatocytes were isolated for *in vitro* culture. After 5 days of culture, DNA content of cultured hepatocytes was analyzed by FACS. (E) Ploidy distribution ratio in the daughter cells was showed as means ± S.D. *, $p < 0.05$; **, $p < 0.01$; Scale bar, 50 μm.

**Supplementary figure 5. Human hepatocyte senescence, polyploidy and transplantation.**

(A) *In situ* staining of γ-H2A.X and Hoechst in young (21-30y) and old (55-65y) human livers. Senescent cells are marked in red. Scale bar, 50 μm. (B) Percentage of γ-H2A.X positive cells in young and old human livers. Data points are means ± S.D. **, $p < 0.01$. (C) Representative FACS histograms showing the DNA content of propidium-iodide-stained nuclei from young and old human livers. (D) The percentages of 2c, 4c and 8c hepatocytes in young and old human livers. Data are presented as the means ± S.D. **, $p < 0.01$. (E, F) Young (E) and old (F) human hepatocytes were transplanted into $Fah^{-/-}Rag\text{-}2^{-/-}$ mice and sacrificed after 8 weeks of repopulation. Repopulated

human hepatocytes in recipient livers were stained by human-specific anti-ALB antibody. Scale bar, 1 mm.

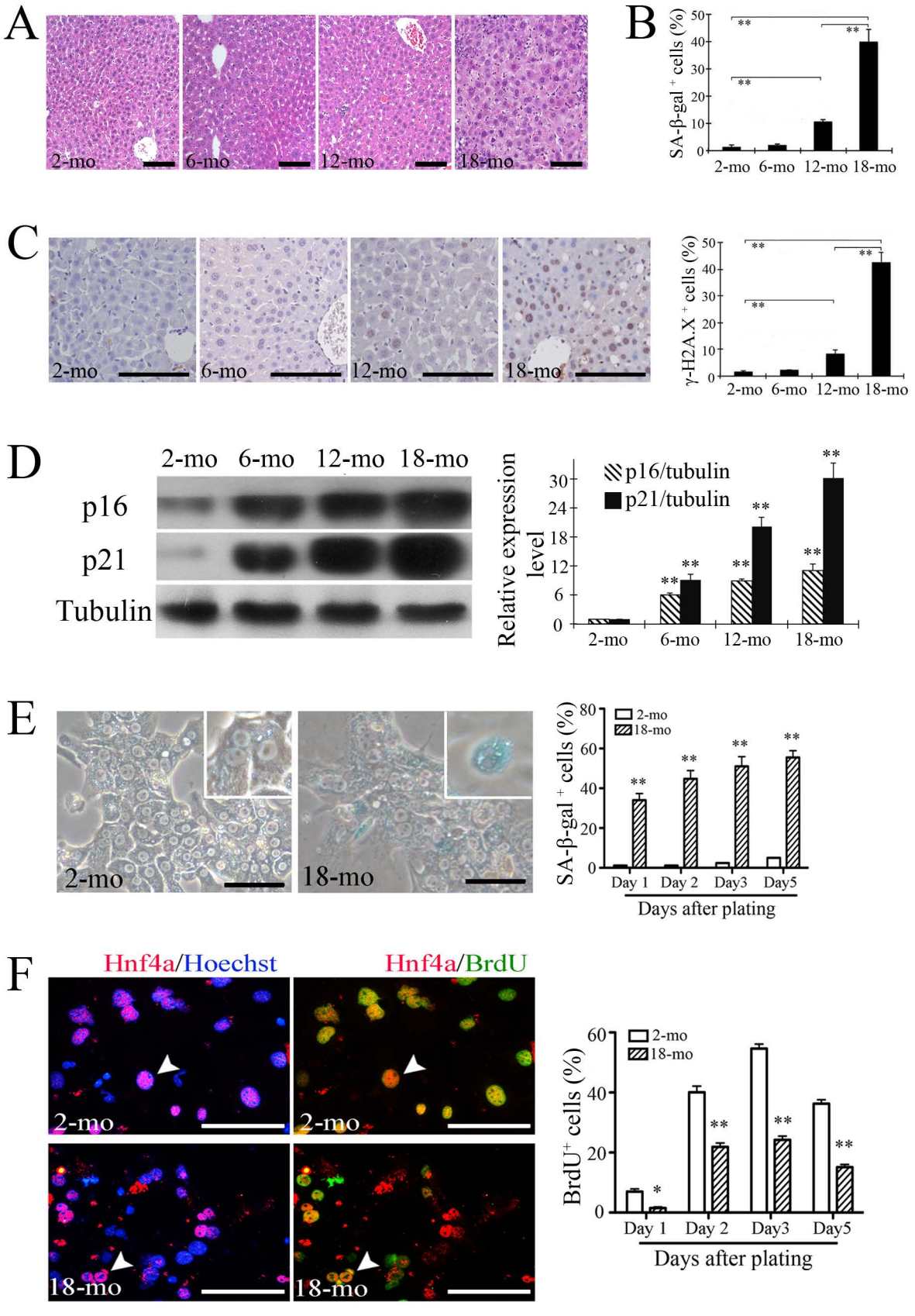
A
2-mo
6-mo
12-mo
18-mo
B
SA-β-gal + cells (%)
2-mo 6-mo 12-mo 18-mo
C
2-mo
6-mo
12-mo
18-mo
γ-H2A.X + cells (%)
2-mo 6-mo 12-mo 18-mo
D
2-mo 6-mo 12-mo 18-mo
p16
p21
Tubulin
Relative expression level
p16/tubulin
p21/tubulin
2-mo 6-mo 12-mo 18-mo
E
2-mo
18-mo
SA-β-gal + cells (%)
2-mo
18-mo
Day 1 Day 2 Day3 Day5
Days after plating
F
Hnf4a/Hoechst
Hnf4a/BrdU
2-mo
2-mo
18-mo
18-mo
BrdU+ cells (%)
2-mo
18-mo
Day 1 Day 2 Day3 Day5
Days after plating

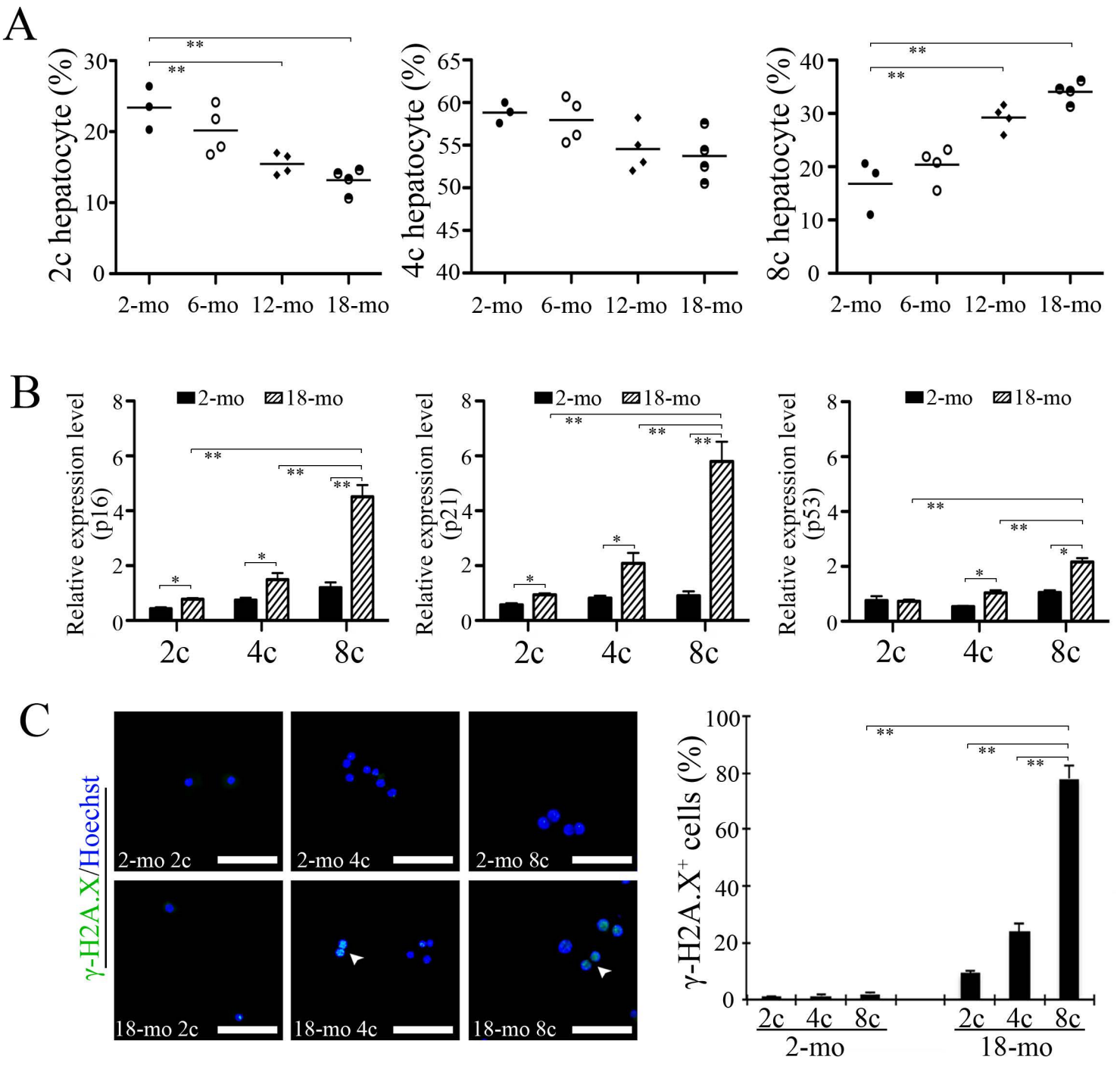
A
2c hepatocyte (%)
4c hepatocyte (%)
8c hepatocyte (%)
2-mo
6-mo
12-mo
18-mo
B
Relative expression level (p16)
Relative expression level (p21)
Relative expression level (p53)
2-mo
18-mo
2c
4c
8c
C
γ-H2A.X/Hoechst
2-mo 2c
2-mo 4c
2-mo 8c
18-mo 2c
18-mo 4c
18-mo 8c
γ-H2A.X+ cells (%)
2-mo
18-mo

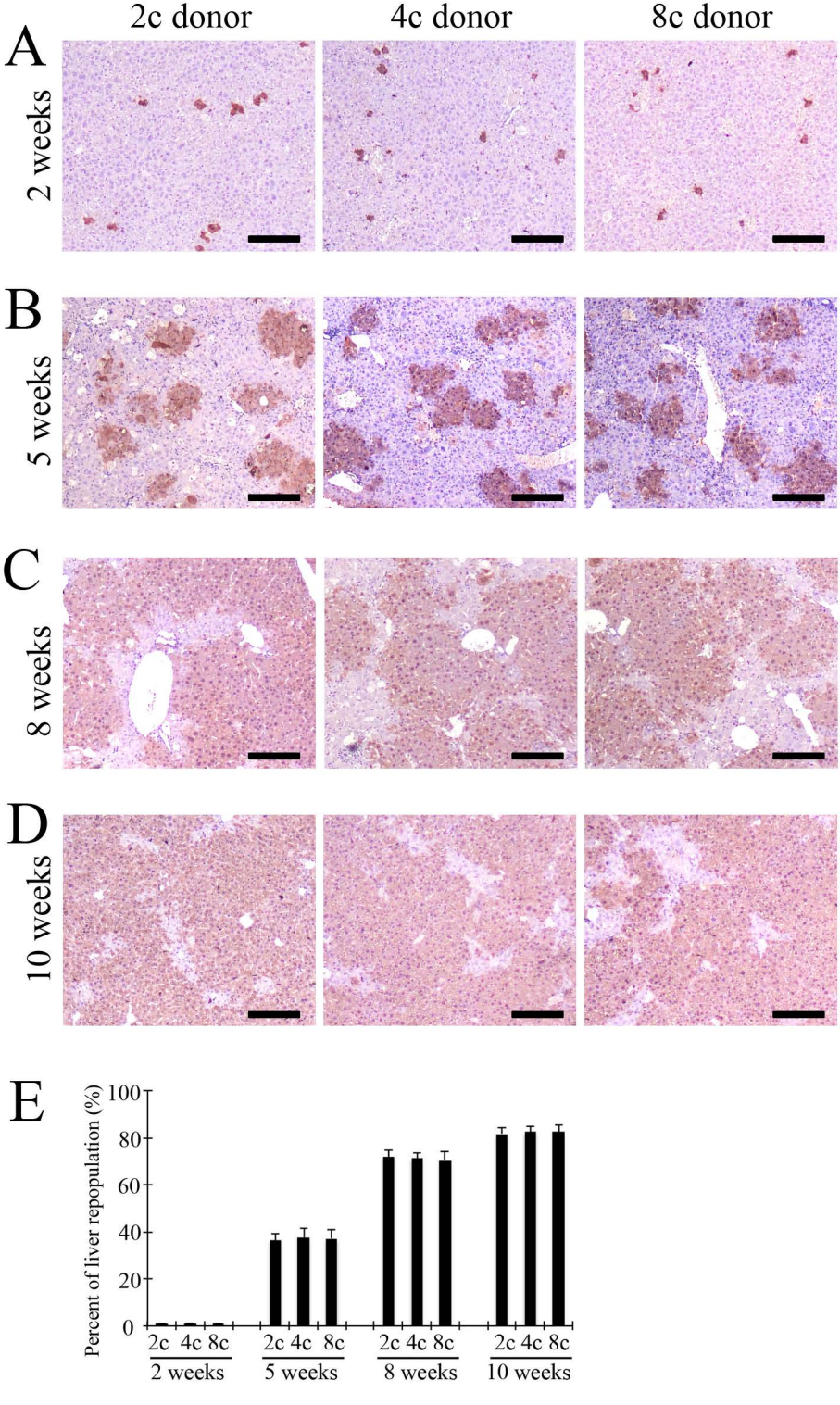
2c donor
4c donor
8c donor
A
2 weeks
B
5 weeks
C
8 weeks
D
10 weeks
E
Percent of liver repopulation (%)
100
80
60
40
20
0
2c 4c 8c
2 weeks
2c 4c 8c
5 weeks
2c 4c 8c
8 weeks
2c 4c 8c
10 weeks

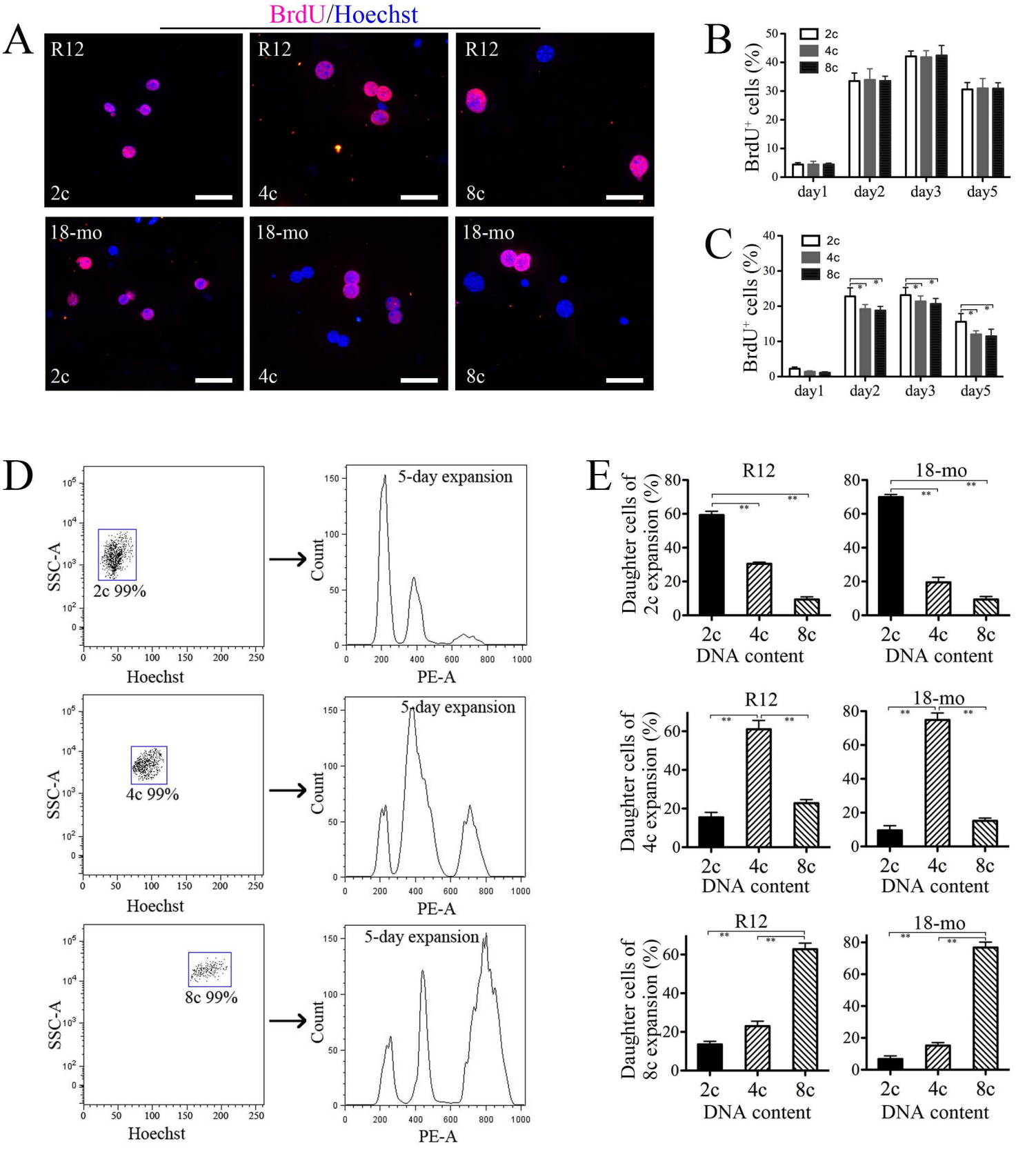
A
BrdU/Hoechst
R12
2c
4c
8c
18-mo
B
BrdU+ cells (%)
2c
4c
8c
day1
day2
day3
day5
C
BrdU+ cells (%)
D
SSC-A
Hoechst
2c 99%
4c 99%
8c 99%
5-day expansion
Count
PE-A
E
Daughter cells of 2c expansion (%)
Daughter cells of 4c expansion (%)
Daughter cells of 8c expansion (%)
DNA content

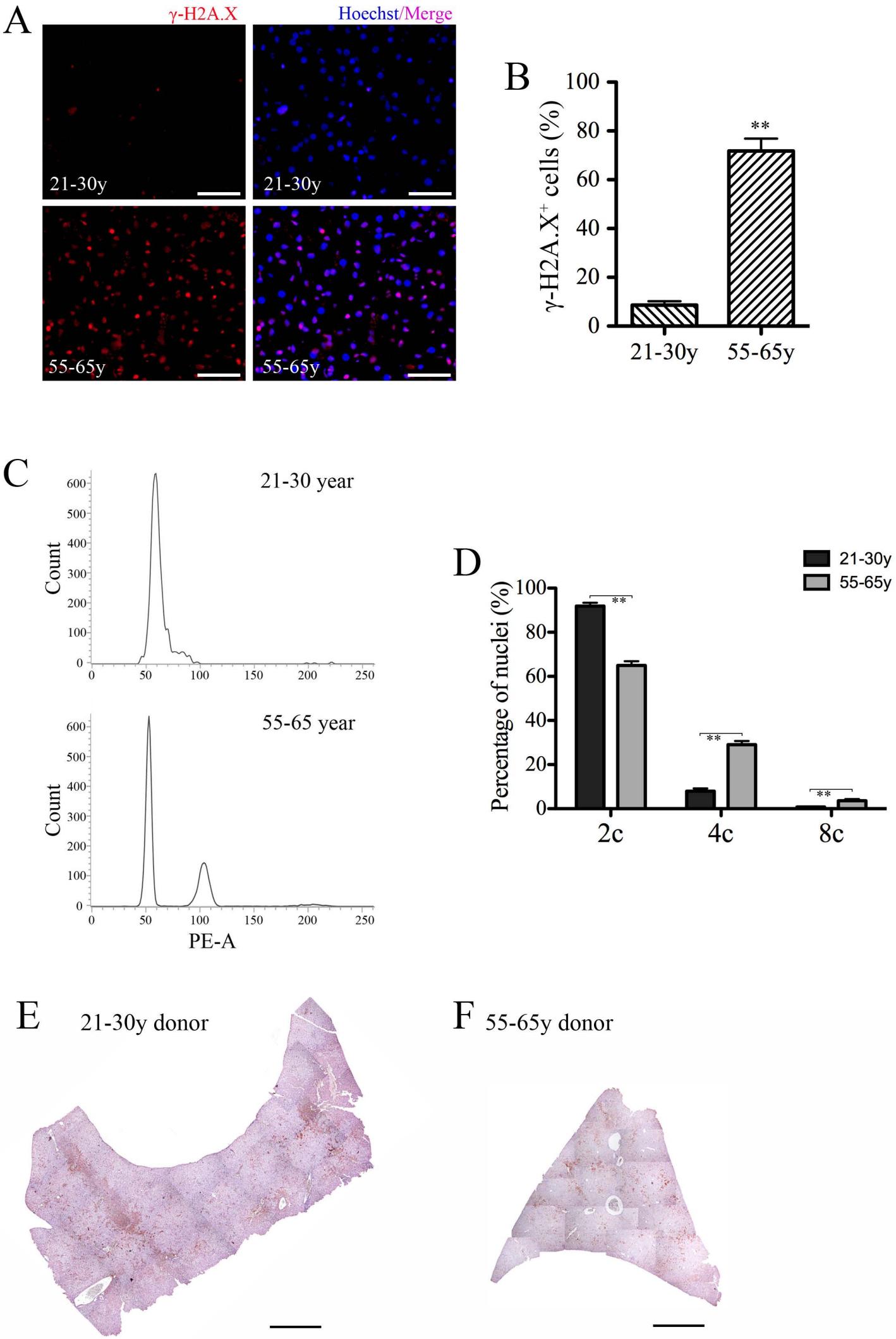
A
γ-H2A.X
Hoechst/Merge
21-30y
21-30y
55-65y
55-65y
B
γ-H2A.X+ cells (%)
100
80
60
40
20
0
**
21-30y
55-65y
C
21-30 year
Count
600
500
400
300
200
100
0
0
50
100
150
200
250
55-65 year
Count
PE-A
D
21-30y
55-65y
Percentage of nuclei (%)
**
**
**
2c
4c
8c
E
21-30y donor
F
55-65y donor